

# **Clinical and Genetic Study of Hereditary Skeletal Disorders in Three Consanguineous Families**



by

**Muhammad Ilyas**

Department of Biochemistry

Faculty of Biological Sciences

Quaid-i-Azam University Islamabad, Pakistan

2023

# Clinical and Genetic Study of Hereditary Skeletal Disorders in Three Consanguineous Families



A thesis submitted in complete fulfillment of the requirements

for the degree of Master of Philosophy

In

Biochemistry/Molecular Biology

by

**Muhammad Ilyas**

Department of Biochemistry

Faculty of Biological Sciences

Quaid-i-Azam University Islamabad, Pakistan

2023

DEDICATED TO  
MY BROTHER WHOEVER WISHES TO SEE MY  
SUCCESS

&

FATHER (LATE) & MOTHER WHOSE  
PRAYERS, LOVE & AFFECTION ARE A  
SOURCE OF STRENGTH FOR ME IN EVERY  
STEP OF LIFE

## **Declaration**

I hereby declared that the work presented in this thesis is my own work. It is written and composed by me. No part of this thesis has been previously published for any other degree or certificate.

**Muhammad Ilyas**

DRSML QAU

# Table of Contents

<i>Acknowledgment</i> .....	v
<b>LIST OF FIGURES</b> .....	ii
<b>LIST OF TABLES</b> .....	vii
<b>ABBREVIATIONS</b> .....	viii
<b>ABSTRACT</b> .....	12
<b>1. INTRODUCTION</b> .....	1
<b>1.1 Human Skeleton</b> .....	1
<b>1.2 Morphology of the Human Bone</b> .....	1
<b>1.3 Skeletogenesis</b> .....	2
<b>1.4 Embryonic lineage of Skeleton</b> .....	2
<b>1.5 Axial Skeleton</b> .....	2
<b>1.6 Craniofacial skeleton</b> .....	3
<b>1.7 Appendicular skeleton</b> .....	4
<b>1.8 Cartilage Anatomy</b> .....	5
<b>1.9 Molecular Pathways involved in Bone Development</b> .....	5
<b>1.9.1 BMP/TGF- Pathway</b> .....	5
<b>1.9.2 Ca Signaling</b> .....	5
<b>1.9.3 Wnt Signaling Pathway</b> .....	5
<b>1.9.4 FGF pathway</b> .....	6
<b>1.9.5 Notch signaling</b> .....	6
<b>1.10 Skeletal Dysplasia</b> .....	6
<b>1.10.1 Classification of Skeletal Disorders</b> .....	7
<b>1.10.2 Lysosomal storage disorder</b> .....	8
<b>1.10.3 Mucopolysaccharidosis</b> .....	9
<b>1.13 Acromesomelic dysplasia</b> .....	13
<b>1.13.1 Acromesomelic Dysplasia Grebe-type (AMDG)</b> .....	13
<b>1.13.2 Acromesomelic dysplasia Hunter–Thompson type</b> .....	13
<b>1.13.3 Acromesomelic dysplasia Maroteaux type</b> .....	14
<b>1.11 Spondylocostal dysostosis</b> .....	14
<b>1.12 Genetic Heterogeneity of Spondylocostal Dysostosis</b> .....	15
<b>1.14 Aims and Objectives</b> .....	15
<b>2. Materials and Methods</b> .....	17
<b>2.1 Study Subject and ethical approval</b> .....	17
<b>2.2 Pedigree design</b> .....	17

2.3 Blood Sample Collection.....	17
2.4 Genomic DNA Extraction.....	17
2.4.1 Extraction of Genomic DNA by phenol-chloroform method .....	18
2.5. Agarose Gel Electrophoresis .....	20
2.6 Homozygosity Mapping.....	21
2.7 Polymerase chain reaction (PCR).....	21
2.8 Polyacrylamide Gel electrophoresis (Vertical Gel) .....	23
2.9 Gene sequencing.....	24
2.9.1 First Sequencing PCR.....	24
2.10 Analysis of Sequenced data .....	25
3. RESULTS.....	33
3.1 Families Descriptions.....	33
3.1.1 Family A.....	33
3.1.2 Family B.....	33
3.1.3 Family C.....	33
3.2 Mapping of Genes Involved in Hereditary Skeletal Disorders .....	34
3.3 Mapping of Genes Involved in Hereditary Skeletal Disorders .....	38
4. Discussion.....	54
5.References.....	58

## *Acknowledgment*

Foremost, I am very thankful to “Allah Almighty”, who blessed mankind with a repertoire of knowledge and wisdom, to unravel the mysteries and unseen facts of nature. Countless salutations are upon Holy Prophet (P.B.U.H), the most perfect among ever born on earth, which is forever a torch of guidance and knowledge for humanity.

I would like to present my special gratitude to my respected father (late) and mother, an ocean of love and prayer. It would be my immense pleasure to present a salute of honor to my elder sisters and brother.

I owe special thanks to my brothers. Being the youngest brother, they always provided me with an excellent educational environment that gave a new direction to my way of thinking. Their discussion on the latest research areas motivated me in the research field.

I would like to express my sincere gratitude to my honorable supervisor **Prof. Dr. Imran Ullah** and **Prof. Dr. Wasim Ahmad** Department of Biochemistry, Quaid-i-Azam University, Islamabad, for their guidance, support, kind interest and valuable suggestions in my entire research journey. Being extraordinary researchers, their ideas inspired and forced me to carry on research in the field of human genetics.

I owe special thanks to **Prof Dr. Irum Murtaza**, Chairperson, Department of Biochemistry, Quaid-i-Azam University, Islamabad. She always motivated and encouraged me all the time during my stay at the department.

It would give me a lot of pleasure to mention my honorable seniors **Kifayat Ullah, Hammal khan, Amjad Ali Tanoli, Sohail Ahmed, Javid Ahmed, Abdullah, Rubab Raza. Fatih ullah, Hajira Fayyaz, Attiya, Bushra Khan, and Tahir Sheykh** for their kind support, valuable discussions, and encouragement made possible this achievement. But among them, **Kifayat Ullah** stands out because he is not only my senior and friend but also treats me like a younger brother, without his help and cooperation my work, though not impossible, would be difficult.

I acknowledge the friendly and cooperative attitude of my class fellow **Zumar Fatima** and juniors for the respect they give me and for their moral support.

I am particularly debited to my friends **Waqar Ahmed, Zahid, Hassan Khan** and **Salman Khan** who always help me in difficult times.

I wish to convey my greetings to my uncle, sisters, and brother Umair Khan for their prayers, support, and acknowledgments that made my research work possible. I have no words to express my feelings for my elder brother Abdullah who compromises a lot during my studies. He is more likely a friend than a brother to me, without him I am nothing.

Last but not least I convey my heartiest thanks to the departmental clerical staff especially **Mr.Tariq, Mr.Fayyaz, and Mr. Shehzad** for their services to students.

**Muhammad Ilyas**



## LIST OF FIGURES

Figure No.	Title	Page No.
<b>Figure 3.1</b>	Pedigree of family A having an autosomal recessive inheritance pattern	35
<b>Figure 3.2</b>	Pedigree of family B having an autosomal recessive inheritance pattern.	36
<b>Figure 3.3</b>	Pedigree of family C having an autosomal recessive inheritance pattern.	36
<b>Figure 3.4</b>	Affected member of family C showing abnormality of chest bone, scapula deformity, and asymmetric body stature.	37
<b>Figure 3.5</b>	Affected individual in family C exhibiting pectus carinatum and showing scapular dyskinesis (B, D).	37
<b>Figure 3.6</b>	Results of the <i>GALNS</i> flanking microsatellite markers in family A	39
<b>Figure 3.7</b>	Results of the <i>NPR2</i> flanking microsatellite markers in family A	40
<b>Figure 3.8</b>	Results of the <i>DLL</i> flanking microsatellite markers in family B.	41

<b>Figure 3.9</b>	Results of the <i>TBX6</i> flanking microsatellite markers in family B	42
<b>Figure 3.10</b>	Results of the <i>HES7</i> flanking microsatellite markers in family B.	43
<b>Figure 3.11</b>	Results of the <i>RIPPLY2</i> flanking microsatellite markers in family B.	44
<b>Figure 3.12</b>	Results of the <i>LFNG</i> flanking microsatellite markers in family B.	45
<b>Figure 3.13</b>	Results of the <i>MECP2</i> flanking microsatellite markers in family B.	46
<b>Figure 3.14</b>	Results of the <i>DLL3</i> flanking microsatellite markers in family C.	47
<b>Figure 3.15</b>	Results of the <i>MECP2</i> flanking microsatellite markers in family C.	48
<b>Figure 3.16</b>	Results of the <i>TBX6</i> flanking microsatellite markers in family C.	49
<b>Figure 3.17</b>	Results of the <i>HES7</i> flanking microsatellite markers in family C.	50
<b>Figure 3.18</b>	Results of the <i>RIPPLY2</i> flanking microsatellite markers in family C.	51

<b>Figure 3.19</b>	Results of the <i>LFNG</i> flanking microsatellite markers in family C.	52
--------------------	---	----

DRSML QAU

## LIST OF TABLES

Table No	Title	Page No
Table 2.1	Composition of the Solutions used for DNA Extraction	19
Table 2.2	PCR Reaction Mixture	22
Table 2.3	Composition of Polyacrylamide Gel	23
Table 2.4	List of the Microsatellite Markers	26
Table 2.5	Primers for <i>NPR2</i> Exons Amplification	27
Table 2.6	List of the Microsatellite Markers of Family C	28
Table 2.7	Primers for <i>NPR2</i> Exons amplification	29

## ABBREVIATIONS

%	Percentage
AER	Apical ectodermal ridge
AMD	Acromesomelic dysplasia
AMDG	Acrosomesomelic dysplasia, Grebe type
AMDM	Acromesomelic dysplasia Maroteaux type
APS	Ammonium persulphate
Bp	Base pair
C	Degree centigrade
cGICs	Cyclic nucleotide-regulated ion channels
cGKI	cGMP-dependent protein kinases I
cGKII	cGMP-dependent protein kinases II
cGMP	Cyclic guanosine monophosphate
Cm	Centi morgan

CNP	Type-C natriuretic peptide
CS	Chondroitin sulfate
<i>DLL3</i>	<i>Delta like 3</i>
dNTPs	Deoxyribonucleic acid
EBP	Elastin-binding protein
EDTA	Eyline diamine tetra acetate
F	Forward
GALNS	N-acetylgalactosamine-6-sulfate sulfatase
<i>GDF5</i>	Growth Differentiation Factor 5
INCDB	Intrinsic Constitutional Disorders of Bone
IP3	Inositol-1,4,5-trisphosphate
IRB	Institutional Review Board
LPM	Lateral Plate Mesoderm
LSDs	Lysosomal storage disorders
<i>MECP2</i>	Methyl CpG binding protein 2

mg	Milligram
MgCl <sub>2</sub>	Magnesium chloride
ml	Millilitre
Mm	Milli molar
MPS IVB	Mucopolysaccharidosis Type IVB
MPS IX	Mucopolysaccharidoses type IX
MPSI	Mucopolysaccharidoses type I
MPSII	Mucopolysaccharidoses type II
MPSIII	Mucopolysaccharidoses type III
MPSIV	Mucopolysaccharidoses type IV
MPS's	Mucopolysaccharidoses
MPSVI	Mucopolysaccharidoses type VI
MPSVII	Mucopolysaccharidoses type VII
NaCl	Sodium chloride
NPs	Natriuretic peptides

PAGE	Poly acrylamide gel electrophoresis
PCR	Polymerase chain reaction
pH	Negative log of hydrogen ion concentration
PLC	Phospholipase C
R	Reverse
Rpm	Revolution per minutes
SCDO	Spondylocostal dysostosis
Ta	Annealing temperature
Taq	Thermus aquaticus
TBE	Tris-Borate-EDTA
TEMED	N, N, N, N Tetra methyl ethylene diamine
ul	Microliter
UV	Ultraviolet,
v/v	Volume by volume
ZPA	Zone of Polarizing Activity



## ABSTRACT

Skeleton is an organ system performing numerous multipurpose functions. Number of signaling pathways and genes are involved in the articulate and precise frame work of bones (skeleton). Any alteration/mutation(s) in these signaling pathways and respective gene(s) may result in osteochondrodysplasias/skeletal dysplasia or dystosis. To date, about 461 congenital skeletal dysplasia have been reported and classified into 42 groups. In the present study three consanguineous families of Pakistani origin exhibiting autosomal recessive hereditary skeletal underlying characteristic features of Acromesomelic dysplasia (Family A) and spondylocostal dysostosis (B, C) disorders were studied. Homozygosity mapping technique was used to find out genes responsible for skeletal disorders in these families (A, B and C).

Homozygosity mapping of known loci harboring genes for Acromesomelic dysplasia showed linkage to *NPR2* gene (9p13.3) in family A. After linkage confirmation, all the exons were subjected to sanger sequencing. Sequencing data analysis revealed no pathogenic variant in 15 exons suggesting that variant can be in any of the remaining six exons. The Family B and C were subjected to homozygosity mapping of known loci harboring genes for spondylocostal dysostosis and the markers failed to show any homozygous pattern for alleles. This suggests the involvement of some other pathogenic genes that are contributing to the phenotypes of the patients. In conclusion, we could not identify the causative variant in the sequenced exons of *NPR2* gene which suggests the presence of causative variants in remaining exons in family A. The family B and C did not establish any linkage to the known genes underlying the phenotypes of these disorders; therefore, we presume the involvement of a novel gene/s.

## 1. INTRODUCTION

### 1.1 Human Skeleton

The skeleton is an organ system made up of two connective tissues: cartilage and bone. While maintaining its fundamental purpose of support and movement, skeleton also performs secondary functions like protecting critical organs, serving as a storehouse of minerals like calcium and phosphate. Bone is the toughest kind of connective tissue consisting of osteoblast, osteoclast, and osteocytes make up bone. The skeleton is further divided into the axial and appendicular skeletons, which collectively consist of 206 bones. The bones that run the length of the body are called the axial skeleton, whereas the bones in the forelimbs, the hind limbs, the pelvis, and the pectoral girdles are called the appendicular skeleton. (Savarirayan and Rimoin, 2002).

### 1.2 Morphology of the Human Bone

The hard structure of the body's skeleton, the bones, is made of calcified connective tissues. Despite being soft and elastic like its counterpart, cartilage is far less flexible and much more rigid than muscle. In contrast to cartilage, which is formed solely of chondrocytes, the cells in bones are divided into three types: osteoblasts, which are responsible for bone production and mineralization, osteoclasts, which are multinucleated cells and help in the absorption of bone and osteocytes, which are involved in bone turnover (Florencio *et al.*, 2015; Kini and Nandeesh, 2012).

Based on their form, bones are divided into five groups. For instance, Short bones that are almost equal in length and width; and long bones: those that are longer than they are broad; sesamoid bones: bones embedded in tendons; irregular bones: often with complicated shapes; and flat (frontal) bones. The weight of the body is supported by long bones, which also make mobility easier. The majority of the long bones, including those lower and upper limbs are found in the appendicular skeleton.

Short bones, which are often cube-shaped and consist mostly of spongy bones, support the wrist and ankle joints and allow for a very little movement. The different shapes and architecture of irregular bones mean they do not fit into any of the other categories for bones. The complicated shapes of irregular bones aid in protecting interior organs.

For instance, spinal cord is protected by backbone. The cranium covers the brain, while flat bones, which are thin, more or less bent, and flattened, serve as points of attachment for muscles. The effectiveness of the muscle is increased by the sesamoid, a microscopic nodular bone lodged in a tendon that functions as a pulley by altering the pull lines of the tendon in which it inserts. Most sesamoid bones are found in the thumb and toe, whereas some are considerably smaller and found in the hands and feet (Clarke, 2008).

### **1.3 Skeletogenesis**

The process of human bone formation is accomplished by two processes, i.e., intramembranous ossification and endochondral ossification, resulting in the formation of long bones and craniofacial skeletal elements respectively (De Baat *et al.*, 2005). Intramembranous ossification involves the direct differentiation of mesenchymal cells into osteoblasts cells of bones (Savarirayan and Rimoin, 2002), while endochondral ossification involves the replacement of chondrocytes by osteoblasts as a result of differentiation, proliferation and hypertrophy (Kornak and Mundlos, 2003).

### **1.4 Embryonic lineage of Skeleton**

A systematic process known as skeletal modeling or patterning is in charge of ensuring that skeletal primordia develop in the right connection to one another and that the size, shape, and quantity of skeletal parts are specified. Three different places give the origin to the skeleton. The somites give rise to the axial skeleton, which includes the vertebrae and ribs, whereas the lateral plate mesoderm's mesenchymal cells are the source of appendicular skeleton. Most of the bones in skull and face are formed from the neural crest (Kornak and Mondlos, 2003).

### **1.5 Axial Skeleton**

The somites, temporary organizing structures of the growing embryo found on both sides of the neural tube, are the sole source of the axial skeleton, which is made up of the vertebrae and the dorsal section of the ribs. Somites, which come from the paraxial mesoderm, are collections of epithelial cells with a periodic structure (Kornak and Mondlos, 2003).

Defective somitogenesis is known to cause a variety of axial skeleton developmental abnormalities, such as spondylocostal dysostosis (MIM 277300) and Alagille syndrome (MIM 118450). Pathogenic variations in the Notch receptor NOTCH2 or Notch ligand JAGGED1 are the cause of Alagille syndrome. The primary characteristics of Alagille Syndrome are Liver-, cardiac-, and renal abnormalities, butterfly vertebrae, posterior embryotoxon, characteristic facies, ocular abnormalities and intracranial bleeding (Kamath *et al.*, 2018; Brennan and Kesavan, 2017).

A category of very uncommon hereditary illnesses known as spondylocostal dysostosis are characterized by anomalies in vertebral and costal segmentation and, occasionally, visceral deformities. The anomalies associated with spondylocostal dysostosis include dwarfism, rib fusion, butterfly vertebrae, syndactyly, and brachydactyly. (Turnpenny *et al.*, 201; Wang *et al.*, 2011; Beine, 2004). Both autosomal recessive and dominant inheritance patterns exist for SCDO known Notch ligand *DLL3* gene pathogenic sequence polymorphisms induce type 1 SCDO, whereas mutations in *RIPPY2*, *TBX6*, *LFNG*, *HES7*, and *MESP2* cause types 2, 3, 4, 5, and 6 SCDO, respectively. (Sparrow *et al.*, 2008; Takeda *et al.*, 2017; Beine *et al.*, 2004).

### 1.6 Craniofacial skeleton

Neuro crest and mesoderm are the two embryonic origins of the craniofacial skeleton. The structure and molecular processes of the craniofacial skeleton are intricate and unique from those of the body skeleton. The craniofacial skeleton is made up of the two primary structures neurocranium and viscerocranium. The upper and rear of the skull, commonly referred to as the braincase or brainpan, is called the neurocranium. The viscerocranium, also known as the splanchnocranium and located anterior to the brainpan, is made up of many bones that make up the skeleton of the face and jaws. The maxillae, nasal bones, lacrimal bones, zygomatic bones, vomer, ethmoid bone, palatine bones, sphenoid bone, and mandible are all parts of the viscerocranium. (Wilkie and Morriss-kay, 2001; Wei *et al.*, 2017).

Waardenberg syndrome type I and 3, which are classified as auditory pigmentary disorders along with other symptoms including aberrant hair coloring, skin, canthasian

dystopia, and deafness are caused by the *PAX3* gene. *PAX3* is also involved in neural crest patterning (Pingault *et al.*, 2010).

### 1.7 Appendicular skeleton

The lateral plate mesoderm (LPM) cells take role in the formation of the appendicular skeleton. LPM cells multiply and move out from the embryo's flanks to generate the limb buds. These initially undifferentiated cells read signals based on their placements as development proceeds, differentiate into a range of tissues that make up the adult limb, and shape each limb into its ultimate shape (Marin-Llera *et al.*, 2019).

The upper and lower extremities that make up the appendicular skeleton connect to the axial skeleton at the shoulder joint and pelvis. The term "appendicular" is used to describe a protruding part of a vertebrate's body known as appendage. The lower limb comprises two leg bones (fibula and tibia), one femur, one coxal bone, commonly known as the hip bone, fourteen phalanges (distal, intermediate, and proximal), five metatarsals, and seven tarsal bones (ilium, ischium, and pubis). The upper limb has the same number of phalanges (proximal, intermediate, and distal), 5 metacarpals, 8 carpal bones. The appendicular skeletal system is made up of these bones plus a variety of joints and cartilage.

The proximal stylopodial area, the intermediate zeugopod region, and the distal autopod region are the three primary regions of the limb throughout development. In humans, the foot or hand develops from the autopod region, the leg or forearm from the zeugopod region, and the arm or thigh from the stylopod region. Three axes that are controlled by the genetic signal brought on by the patterning process are where the development of the limbs takes place. Proximal-distal (shoulder to finger), anterior-posterior (thumb to little finger), and dorsal-ventral (back to palm) are these three axes (Ahmad *et al.*, 2002).

The apical ectodermal ridge (AER), the non-ridge ectoderm, and other ingrained signaling systems, such as the ZPA (Zone of Polarizing Activity), regulate the completion of the limb bud development. The three axes of appropriate skeletal modelling and development are guided by each signaling mechanism (dorsoventrally, anteroposterior, proximodistal; Ahmad *et al.*, 2022; Towers and Tickle, 2009).

## 1.8 Cartilage Anatomy

The strong connective tissue that is viscoelastic in nature is called cartilage. It is made up of specialized cells called chondrocytes that are found in the matrix's lacunae. Most bones are present at birth in the form of cartilage, which later solidifies into bones. However, certain cartilages are still in their original form (Geister and Camper, 2015). It is categorized into three groups. Hyaline cartilage, which has a bluish-white appearance and is glass-like yet translucent, is found where the ends of the bones meet to create joints. The ear's auricles contain elastic cartilage, which is robust and looks yellow. Ears are kept in form by yellow cartilage, which also gives them flexibility and strength. The third form of cartilage is fibrous, which has a lot of type I and type II collagen fibers and appears white and found in intervertebral disc and in symphysis pubis (Hall, 2005).

## 1.9 Molecular Pathways involved in Bone Development

### 1.9.1 BMP/TGF- Pathway

The major important signaling pathways in osteogenesis is BMP/TGF. The bulk of cellular pathways involved in bone formation throughout mammalian development require BMP/TGF- signaling. Numerous bone illnesses, including osteoarthritis, tumor metastasis, and brachydactyl type A2 are brought on by the disruption of BMP/TGF- signaling (Hayrapeyan *et al.*, 2015).

### 1.9.2 Ca Signaling

In the process of osteoblast differentiation,  $\text{Ca}^{2+}$  signaling is crucial. Through a number of signaling pathways, ATP-dependent  $\text{Ca}^{2+}$  inflow is achieved through Runx2. by increasing  $\text{Ca}^{2+}$  concentration in cytoplasm phospholipase C (PLC) and inositol-1,4,5-trisphosphate (IP3) signaling is achieved.  $\text{Ca}^{2+}$  release occurs from endoplasmic reticulum in this signaling (Hayrapeyan *et al.*, 2015).

### 1.9.3 Wnt Signaling Pathway

The mechanisms of osteoblast development and mineralization are significantly influenced by Wnt signaling. Wnts trigger the activation of minimum three intracellular signaling cascades, example the canonical Wnt/-catenin way, the non-canonical

Wnt/Ca<sup>2+</sup> route, and the Wnt/planar polarity pathway. Numerous studies show that canonical Wnt pathways are essential for bone formation due to their participation in this osteoblast-specific gene markers expression. The activation of Cytoskeletal organization also take place through Wnt signaling (Hayrapeyan *et al.*, 2015).

#### 1.9.4 FGF pathway

The association of the FGF pathway is essential for regulating process of endochondral and intramembranous signaling. The FGF pathway typically promotes osteoblast formation while suppressing osteocyte differentiation. FGF signaling therefore affects osteoblast maturation at different stages (Hayrapeyan *et al.*, 2015).

#### 1.9.5 Notch signaling

Through the action of four NOTCH receptors (NOTCH1-4) and at least five ligands, Notch signaling also inhibits chondrogenesis. During somitogenesis, axial skeleton segmentation depends on Notch signaling. A deficiency in vertebral segmentation, marked by aberrant vertebrae and ribs, results from defective somitogenesis caused by faulty Notch signaling, which results in trunk dwarfism (Guasto and Cormier-Daire, 2021).

### 1.10 Skeletal Dysplasia

Skeletal anomalies may result from irregularities in the major signaling networks (WNT, Notch, Hedgehog, TGF B, etc.) that are crucial to the evolution of the skeletal elements. Numerous skeletal dysplasia is caused by defects in bone production, homeostasis, and mineralization (Marzin and Cormier-Daire, 2020).

Osteodysplasias and dysostoses are two terms used to describe skeletal conditions caused by abnormalities in the bony component of the skeleton. Osteodysplasias disrupt bone mineralization and result in osteoporosis and osteopenia, whereas dysostoses only affect a single skeletal component and have a more limited impact. Dysostoses often occur from abnormal skeletal patterning gene activation. (Schramm *et al.*, 2009; Hurst *et al.*, 2005).

Chondrodysplasias are skeletal malformations that often affect the whole appendicular skeleton and are brought on by disruption of the cartilaginous component of the

skeleton. Chondrodysplasias were caused by mutations in organogenesis-related genes (Mortier, 2001).

Large variations in the presentation of skeletal disorders, including the mode of heredity, age at which growth retardation first manifested, radiographic characteristics, inheritance manner, and severity, etc. Skeletal diseases are highly challenging to characterize due to phenotypic heterogeneity (Superti-Furga and Unger, 2010).

### 1.10.1 Classification of Skeletal Disorders

Numerous updates were made to the classification of various skeletal anomalies based on radiological, metabolic, and clinical factors and published by nosology (skeletal dysplasia). INCDB (Intrinsic Constitutional disorders of Bone) was established to develop advanced nomenclature for various skeletal dysplasia, with a primary focus on grouping various metabolic abnormalities, novel syndromes, and other skeletal disorders (Mortier *et al.*, 2019).

No suitable single categorization of these illnesses is conceivable due to their variability. It is required to categorize bone deformity utilizing clinical, radiographic, morphologic, biochemical, and molecular data in a number of dimensions. The interdisciplinary diagnosis of skeletal abnormalities is improved by identifying skeletal components with aberrant size, form, and mineralization patterns. (Rimoin *et al.*, 2007).

It's interesting that multiple phenotypes may arise from mutations in the same gene for many bone illnesses, such as Stickler syndrome and deadly achondrogenesis from COL2A1 mutations. In contrast, comparable abnormalities might result from mutations in other genes. For instance, numerous epiphyseal dysplasias can be caused by mutations in six separate genes (Rimoin *et al.*, 2007; Jakkula, 2005).

Rimoin *et al.* (2007) categorized different bone illnesses based on deficiencies in common proteins, signaling pathways, metabolic processes, and particular bodily organs in order to provide a clear and practical categorization. This classification system classifies the following disorders as belonging to the same category: achondrogenesis, multiple epiphyseal dysplasia, pseudo achondroplasia, osteogenesis imperfect, and metaphyseal dysplasia. These disorders involve defects in extracellular structural



proteins such as COL9A1/2/3, COL1A1/2, COMP and COL10A1. Defects in the tissue non-specific alkaline phosphatase pathway lead to the disorder hypophosphatasia, while irregularities in the diastrophic dysplasia sulphate transporter lead to the disorder achondrogenesis 1B. (Rimoin *et al.*, 2007). Several illnesses, including Mucopolysaccharidoses, Lesch-Nyhan syndrome, Pycnodysostosis, Mucopolidosis II and III and are caused by defects in the metabolism and transport of macromolecules due to the lack of metabolic enzyme (Rimoin *et al.*, 2007).

(Numerous bone diseases are brought on by abnormal cytoskeletal proteins, such as Boomerang dysplasia, Otopalotodigital syndromes I and II, Melnick-Needles, frontometaphyseal dysplasia, Spondylocarpotarsal syndrome, Atelosteogenesis I/III, Larsen syndrome, and, which are caused by defects in actin binding proteins. Different forms of skeletal problems including lysosomal storage diseases are caused by inborn metabolic abnormalities (Rimoin *et al.*, 2007).

According to recent and tenth edition reviewed by (Mortier *et al.*, 2019) 461 disorders were placed in 42 groups based on their clinical, radiological, and/or molecular phenotypes Remarkably, 425/461 (92%) of these illnesses had pathogenic mutations impacting 437 distinct genes.

The category of ciliopathies with significant skeletal damage has replaced the short-rib dysplasia (with or without polydactyly) group. The brachydactylies have been divided into two groups: those with extraskeletal manifestations and those without extraskeletal manifestations as a result of the growing number and complication in the brachydactylies (Bonafe *et al.*, 2015).

### **1.10.2 Lysosomal storage disorder**

Because of a genetic defect that prevents the production or processing of the enzyme(s) required for their breakdown, macromolecules (proteins, polysaccharides, and lipids) accumulate in the lysosomes, which results in lysosomal storage disorders (LSDs). The most prevalent LSD's with skeletal disease are type 1 and 3 Gaucher disease and the mucopolysaccharidosis (MPS's) (Clarke and Hollak, 2015).

### 1.10.3 Mucopolysaccharidosis

Mucopolysaccharidoses (MPS) are genetically inherited metabolic defects that occur due to the defects in the lysosomal enzymes which are then responsible for the degradation of the GAGs. GAGs are sulfated polysaccharides made up of repeating units of disaccharides, galactose, and hexosamines. These GAGs help in the formation of bone, skin, eye corneas, cartilage, and connective tissues. There are four types of mucopolysaccharides which are dermatan sulphate, keratin sulphate, chondroitin sulphate (KS) and heparin sulphate, and. Lysosomal enzymes play important roles in the degradation of GAGs that then help in the normal functioning of the tissues and the ECM. Defects occur in one or more lysosomal enzymes that disturb the normal degradation of GAGs and GAGs are accumulated and as a result function of the cells, tissues, and organs is affected. These accumulated GAGs are then moved into the bloodstream and then with the help of urine move out of the body (Khan *et al.*, 2017). Increased levels of GAGs cause disruption in the development of bone and cartilage, ossification of bones, growth balance. These disruptions then lead to unique structural dysplasia.

#### 1.10.3.1 Classification of Mucopolysaccharidosis

Mucopolysaccharidosis are genetic disease that exhibit X-linked as well as autosomal recessive inheritance. MPS are classified into seven types based on the defect in a specific lysosomal enzyme. Total of eleven lysosomal enzymes are present. The seven categories of MPS are represented as. MPSI, MPSII, MPSIII, MPSIV, MPSVI, MPSVII and MPS IX. In Pakistan MPS I is present most frequently followed by MPS IV, MPS III MPS II is very rare (Cheema *et al.*, 2017). These MPS have different clinical features and severity with each type. These seven types are following:

#### 1.10.3.2 Mucopolysaccharidosis Type I

MPS Type I is divided into three different syndromes and these syndromes mostly show common clinical features (Muenzer, 2004). Defect in the lysosomal enzyme,  $\alpha$ -L-iduronidase (IDUA) cause MPS I that helps in the breakdown of DS and HS. Accumulation of these GAGs disrupts the functions of bones and the brain. Clinical features of MPS I patients include corneal clouding, mental and growth retardation,

hernia, coarse face, kyphosis, scoliosis, hearing problems, and joint contractures (Neufeld, 2001). The prevalence of MPS I is 0.22/100,000 births.

#### **1.10.3.3 Mucopolysaccharidosis Type II**

MPS type II/Hunter syndrome occurs due to the defects in Iduronate-2-sulfatase (I2S) gene that encodes a lysosomal enzyme. I2S causes the breakdown of HS and DS. Only MPS II shows an X-linked inheritance pattern and hence males are affected more. Clinical features of this syndrome include growth and mental retardation, short stature, facial coarsening, joint stiffness, hearing loss, skeletal deformities, macrocephaly, thickening of lips, delay in tooth eruption, sleep apnea, cardiac, and respiratory disturbances, and umbilical hernias (Fesslova *et al.*, 2009; Stapleton *et al.*, 2017). MPS II occurs in approximately 0.45/ 100,000 births.

#### **1.10.3.4 Mucopolysaccharidosis Type III**

MPS type III occurs due to the accumulation of a large amount of HS as the enzyme involved in its breakdown is mutated. A high level of HS then disrupts the normal body functioning and causes Sanfilippo syndrome (Valstar *et al.*, 2008). MPS III is transmitted in an autosomal recessive way. MPS III is classified into four types due to defects in four different lysosomal enzymes., MPS IIIB ( $\alpha$ -N-acetylglucosaminidase), MPS IIID (N-acetyl-glucosamine-6-sulfatase), MPS IIIA (heparan-N-sulfatase) and MPS IIIC ( $\alpha$ -glucosaminidase-acetyltransferase) (Fedele, 2015).

#### **1.10.3.5 Mucopolysaccharidosis Type IV**

MPS type IV or Morquio syndrome was first reported by a pediatrician, L. Morquio (1929) and Brailsford (1929). Symptoms of Morquio syndrome vary from mild to severe. At the time of birth patients with Morquio syndrome look normal and early symptoms appear by the age of two to three years. Classical symptoms are the short trunk, dwarfism, scoliosis, pectus carinatum, knock knee, kyphosis, joint laxity and hypermobility, heart and eye problems, large head, odontoid dysplasia, coarse face, flat bridged nose, abnormal gait with frequent fall and prominent forehead (Tomatsu *et al.*, 2005). Morquio syndrome is a rare disorder and occurs in 1 in every 40,000 live births (Nelson *et al.*, 2003). Morquio syndrome is divided into two types depending on the defects in the normal functions of two lysosomal enzymes. These types are given below.

### 1.10.3.6 Mucopolysaccharidosis Type IVA

MPS IVA (MIM #253000) occurs due to the defect in the GALNS gene which is transcribed into a protein named N-acetylgalactosamine-6-sulfatase which is a lysosomal enzyme. The activity of the enzyme is partially reduced or completely lost in some cases. As a result, GAGs are not degraded and here KS and C6S are accumulated in MPS IVA. The production of KS and C6S primarily occurs in the cartilage and disturbance in their degradation results in their accumulation in the lysosome and ECM. This then disrupts the normal functioning of the bones and cartilage and leads to skeletal abnormalities (Khan *et al.*, 2017). Classical symptoms are the short trunk, dwarfism, scoliosis, pectus carinatum, knock knee, kyphosis, joint laxity and hypermobility, heart and eye problems, large head, odontoid dysplasia, coarse face, flat bridged nose, abnormal gait with frequent fall and prominent forehead (Tomatsu *et al.*, 2005). MPS IVA occurs in 1 in every 640,000 (Nelson *et al.*, 2003). The GALNS gene is present on 16q24.3 and has an approximate length of 50kb. GALNS gene consists of 14 exons and transcribes 2,339 base pairs long messenger RNA that then further translates to form a 522 a.a (Amino acids) long protein (Tomatsu *et al.*, 1991; Nakashima *et al.*, 1994; Fukuda *et al.*, 1996). Total 446 variants are reported in GALNS so far in which missense variants account for 65% of the total variants (Zanetti *et al.*, 2021).

### 1.10.3.7 Mucopolysaccharidosis Type IVB

MPS IVB (MIM #253010) occurs due to a mutation in the gene known as GLB1. GLB1 encodes the  $\beta$ -galactosidase enzyme. The function of the enzyme is completely lost or reduced based on the type of mutation in the GLB1 gene. In the case of MPS IVB, only KS is accumulated in the lysosome and ECM and leads to skeletal defects (Khan *et al.*, 2017). Common features include growth retardation, short trunk, dysostosis, knocking knees, defects in wrists, hips, chest, and ribs, coarsening of the face, respiratory difficulties, sleep apnea, heart diseases, clouding of the cornea, pectus carinatum, genu valgum, kyphoscoliosis, and nervous disabilities in severe cases (Tomatsu *et al.*, 2011; Khan *et al.*, 2017). MPS IVB occurs in approximately 1 in every 250,000 to 1,000,000 births (Baehner *et al.*, 2005). GLB1 is located on chromosome 3p22.3 and is 62.5 kb long and consists of 16 exons. Alternate splicing in GLB1 results in a 2.5kb messenger

RNA transcript which encodes  $\beta$ -galactosidase and a shorter transcript of 2 kb size which encodes an elastin-binding protein (EBP; Santamaria *et al.*, 2007). Total 252 pathogenic variants have been reported in the GLB1 underlying MPS IV B. Out of these 252 mutations more than 86% mutations are missense mutations (Sohn *et al.*, 2012).

#### 1.10.3.8 Mucopolysaccharidosis Type VI

MPS type VI transfers in an autosomal recessive pattern and is caused by the defects in the enzyme, arylsulphatase B (ARSB). ARSB is involved in the breakdown of DS and CS. Any defect in ARSB results in the accumulation of the DS and CS in the lysosomes and connective tissues (Valayannopoulos *et al.*, 2010). Common clinical features found in this disorder are growth retardation, cardiac and respiratory abnormalities, coarse face, skeletal dysplasias, and joint stiffness (Neufeld, 2001).

#### 1.10.3.9 Mucopolysaccharidosis Type VII

MPS type VII is a heterogeneous and rare storage disorder and inherited in an autosomal recessive way. MPS VII occurs due to defects in the activity of the  $\beta$ -glucuronidase (GUS) gene (Linker *et al.*, 1995). GUS helps in the breakdown of glucuronic acid residues from the DS, HS, and CS. Any defect in GUS leads to the storage of these GAGs in the connective tissues, spleen, brain, lungs, and heart (Montano *et al.*, 2016). Symptoms of MPS VII include skeletal abnormalities, respiratory and cardiac disorders, coarse face, and enlargement of the liver and spleen (Cadaoas *et al.*, 2020).

#### 1.10.3.10 Mucopolysaccharidosis Type IX

The incidence of MPS IX is very low among all other MPS and shows an autosomal inheritance pattern. MPS IX occurs due to defects in the hyaluronidase enzyme that help in the breakdown of hyaluronic acid. *HYAL1* gene is mutated which encodes hyaluronidase enzyme (Triggs-Raine *et al.*, 1996). Only four cases of MPS IX. Clinical features of this syndrome may include cysts, ear infections, short stature, and cleft palate (Khan *et al.*, 2017).

### 1.13 Acromesomelic dysplasia

Acromesomelic dysplasia (AMD) is a group of autosomal recessive form of skeletal disorders characterized by disproportionate of skeletal element, mostly affecting forearms, forelegs (Middle segments) and hands, feet (distal segments) of the skeletal system. Both solitary (non-syndromic) and syndromic types of AMD exist. It has a syndromic form that is linked to disorders of the respiratory, genital, cardiac, and nervous systems (Khan *et al.*, 2016). The various types of Acromesomelic dysplasia are

#### 1.13.1 Acromesomelic Dysplasia Grebe-type (AMDG)

Acromesomelic dysplasia, Grebe type (AMDG; OMIM 200700) is a rare skeletal disorder, with autosomal recessive mode of inheritance causes severe dwarfism with prominent micromelia, deformities of the upper and lower limbs that vary in severity along the proximodistal, axisproximal and middle phalanges are absent, the middle long bones are small and malformed, the carpal and tarsal bones are fused, and there are many metacarpal bones. The afflicted individuals' intelligence and facial traits are not affected (Martinez-garcie *et al.*, 2016; Khan *et al.*, 2016).

The *CDMP1* gene has been linked to AMDG via mutations. This gene, which is found on chromosome 20q11.22, is mostly expressed in cartilaginous tissues of growing long bones and farther-reaching parts of the appendicular skeleton. Growth Differentiation Factor 5 (*GDF5*), is member of the secreted signaling molecule superfamily of transforming growth factor beta, is encoded by *CDMP1*. *GDF5* is involved in the regulation of limb patterning, joint development, and distal bone growth by stimulating the early stages of chondrogenesis, which increase cellular adhesion and then chondrocytic proliferation. biallelic sequence variants in the receptor of (*GDF5*) bone morphogenetic protein receptor-1b (*BMPRI1B*) also cause AMDG (Martinez-garcie *et al.*, 2016, Umair *et al.*, 2017; Ullah *et al.*, 2018).

#### 1.13.2 Acromesomelic dysplasia Hunter–Thompson type

Acromesomelic dysplasia Hunter–Thompson type (AMDH, MIM 201250), phenotypes include shortening of the limbs. Lower limbs are more affected than the upper limbs. Anomalies in the upper limbs include hands with short phalanges and metacarpals, a short humerus, and a curved radius and ulna, while those in the lower limbs include

short femurs, tibias, and fibulas as well as dislocated ankles. Most severely impacted are the intermediate and distal limbs. *GDF5* biallelic mutations that induce AMDH (Ullah *et al.*, 2018).it is also mapped on chromosome 20q11.22 (Khan *et al.*, 2016).

### 1.13.3 Acromesomelic dysplasia Maroteaux type

AMDM is an autosomal recessive disorder Disproportionately small stature, and a discernible shortening of distal and middle and skeletal parts are among the clinical characteristics. Short ulnas with hypoplastic distal ends were seen in AMDM patients' radiographic characteristics. Typically, a dolichocephalic skull without related facial or mental problems is characterized by a short trunk and lower vertebral height (Umair *et al.*, 2015).

prevalence is 1/1,000,000 birth. Mutation in gene natriuretic peptide receptor-2 (*NPR2*) is responsible for AMDM. By interacting with natriuretic peptide receptors on cell surfaces, natriuretic peptides (NPs), a family of hormones, maintain many physiological processes which include heart development, endochondral ossification (NPRs) axonal pathfinding and blood pressure. There are three distinct subtypes of NPRs (A, B, and C). NPR-B is expressed in a variety of organs and cell types, including the uterus, brain, heart, and blood vessels. In a number of tissues Locally, NPR-B performs a paracrine and/or autocrine regulatory role. It is a type-C natriuretic peptide (CNP) receptor. When *NPR2*'s membrane-bound guanylyl cyclase binds to its ligand, C-type natriuretic peptide, it produces the secondary messenger cyclic guanosine monophosphate (cGMP) (Khan *et al.*, 2016; Geister *et al* 2015).

### 1.11 Spondylocostal dysostosis

Spondylocostal dysostosis (SCDO, MIM 277300) is a group of vertebral malsegmentation syndromes resulting from axial skeleton abnormalities with reduced stature. Multiple hemivertebrae, rib fusions, deletions, and non-progressive kyphoscoliosis are characteristics of SD. There have been reports of both autosomal dominant and autosomal recessive patterns of inheritance, it occurs once in 40,000 births. (Bolman *et al.*, 2000). The subtype is determined by the discovery of biallelic pathogenic mutations in one of the six genes—*DLL3*, *TBX6*, *HES7*, *MESP2*, *LFNG*, and *RIPPLY2*—known to cause autosomal recessive SCDO (Turnpenny *et al.*, 2017).

### 1.12 Genetic Heterogeneity of Spondylocostal Dysostosis

Different types of SCDO are SCDO1 which is caused due to mutation in *DLL3* genes (602768) mapped on chromosome 19q13. SCDO2 (608681), gene positioned on chromosome 15q26 is because of mutation in the *MESP2* gene; SCDO3 (609813) is due to mutation in *LFNG*. The gene is positioned on chromosome 7p22. SCDO4 (613686), occur due to mutation in the *HES7* gene. *HES7* gene is located on chromosome 17p13, 16p11 is the locus of the *TBX6* gene, and mutation in this gene is responsible for SCDO5 (122600), and SCDO6 (616566), the gene involved in mutation is *RIPPLY2* gene set on chromosome 6q14.

### 1.14 Aims and Objectives

In the current work, three families with hereditary skeletal disorders from Pakistan were selected for the identification of genetic variants causing skeletal disorders. Three families presented skeletal disorders associated with Acromesomelic dysplasia, and Spondylocostal dysostosis.



DRSML QAU

# **Chapter 02**

## **Materials and Methods**

## 2. Materials and Methods

### 2.1 Study Subject and ethical approval

Three Pakistani families (A, B and C) with skeletal disorder and autosomal recessive mode of inheritance were collected from different regions of Pakistan. To conduct the research, ethical approval was obtained from the Institutional Review Board (IRB) of QAU, Islamabad.

### 2.2 Pedigree design

After interviewing the elders of the families, Pedigrees were designed according to the standard method proposed by Bennet *et al.* (1995). Circles represents females while squares represent males. Affected individuals are represented by filled circles and squares. The generation numbers and individual numbers have been shown by Roman numbers and Arabic numbers respectively. A circle or square crossed by a line indicates the deceased individuals in the family. The consanguineous union of the parents has been shown by a double line.

### 2.3 Blood Sample Collection

For extraction of blood (4-6 ml), 10 ml sterilized syringes (BD 0.8 mm x 38mm 21 G x 1 ½ TW, Franklin lakes, USA) were used. Sample (blood) was collected from the a normal and affected members. The blood was then transferred to potassium containing EDTA tubes (BD Vacutainer K3 EDTA, Franklin Lakes NJ, USA). At 4C the EDTA tubes were stored.

### 2.4 Genomic DNA Extraction

In our lab, we use the following two methods for Genomic DNA extraction;

- **Phenol-chloroform method.**
- **Extraction via commercially available kits (Sigma-Aldrich MO, USA).**

In our study, we have used the conventional phenol-chloroform method for genomic DNA extraction.

### 2.4.1 Extraction of Genomic DNA by phenol-chloroform method

Extraction through phenol-chloroform method requires two days.

#### Day 1st

In the first step, 700  $\mu$ l of blood was taken, equal volume of sol A was added and mixed in 1.5 ml Eppendorf tube by gentle vortexing 4 to 6 times. After mixing, Eppendorf tube was incubated for about 1 hour at room temperature. After incubation, centrifuge the Eppendorf tube for 1 min at 13000 rpm (Eppendorf Microfuge, 5415D, USA). In the third stage, after discarding the supernatant the nuclear pellet was re-suspended in 500  $\mu$ l of solution A. Once again, the pellet was centrifuged for one minute at 15,000 rpm after being dissolved in Solution A. Re-suspended the nuclear pellet in 400  $\mu$ l of solution B and discard the supernatant. Finally, we add, in the Eppendorf tube holding the pellet, add 10  $\mu$ l of proteinase k and 17  $\mu$ l of SDS (20%). Then the samples were placed in an incubator overnight at 37°C.

#### Day 2<sup>nd</sup>

The next day, the samples were mixed to 500  $\mu$ l of new mixture of solutions C and D (250  $\mu$ l Sol-C and 250  $\mu$ l Sol-D), and centrifuged for at 10 min 13,000 rpm. Two different layers were formed after centrifugation. DNA-containing material from the top layer was pipette-picked and transferred to fresh Eppendorf tubes. The Eppendorf tubes holding the DNA were then filled with 500  $\mu$ l of Solution-D and again centrifuged for 10 min at 13,000 rpm (Tab 2.1). Once more, the top layer was removed with a pipette and placed in fresh Eppendorf tubes. The Eppendorf tubes holding the DNA were then filled with 500  $\mu$ l of cold isopropanol and 55  $\mu$ l of 3M sodium acetate (pH 6), and the Eppendorf were gently inverted several times to precipitate the DNA. To precipitate the DNA into a pellet, the Eppendorf tubes were once again centrifuged for 10 minutes at 13,000 rpm. Once more, the supernatant was discarded, and 200  $\mu$ l of cooled 70% ethanol was used to wash the particle. After carefully discarding the ethanol, the DNA was dried for 7–12 min at 45°C in concentrator 5301 (Eppendorf, Hamburg, Germany). Finally, after incubating the DNA for an overnight period at 37°C in an incubator, it was dissolved in 150  $\mu$ l of Tris-EDTA (TE) buffer. Stock DNA was stored at 4°C.

**Table 2.1 Solutions composition used for DNA Extraction**

<b>Solution A</b>	Sucrose 0.32M, Mgcl <sub>2</sub> 5Mm, Tris (PH 7.5), 1% (v/v) triton x-100.
<b>Solution B</b>	EDTA (PH 8.8) 2mM, NaCl 400mM, Tris (PH 7.5) 10Mm.
<b>Solution C</b>	Saturated phenol
<b>Solution D</b>	chloroform, Isoamyl-alcohol at 24:1 volume
<b>20% SDS</b>	10g in 50 ml water
<b>10X TBE</b>	Tris 0.89M, 0.025M Borate, EDTA PH 8.3
<b>Bromophenol blue</b>	40g Sucrose, bromophenol blue (0.25g).

#### 2.4.2 kit Method

Gene Elute Blood Genomic kit (Sigma-Aldrich, Cat. 2010-1, St. Louis, USA) is used for DNA extraction. The following steps are carried out in the extraction of DNA through the kit method.

##### (a) Lysis Step

200 ml of whole blood, 20 ul of proteinase K, and 200 ml of lysis solution C were poured in a 1.5 ml micro centrifuge tube, vortex for about 15 seconds, and then the tube was put in a thermoblock for 15 minutes at 55 °C.

**(b) Binding Step**

A Gene Elute Miniprep Binding column was filled with 500  $\mu$ l of the column preparation solution, and it was centrifuged for 1 min at 12,000 rcf. The flow-through was removed, and 200  $\mu$ l of 100% ethanol were added to the lysate before being transported to the column. A fresh collecting tube was used to hold the column after it had been centrifuged at 6500 rcf for 1 min.

**(c) Washing step**

After washing the column with 500  $\mu$ l of prewash solution (WB1), it was centrifuged at 6500 rcf for one min. A new collecting tube was used to hold the column. To the column, add 500  $\mu$ l of wash buffer II (WB2), and centrifuge for three minutes at 12,000–16,000 rcf. Put the collecting tube in the trash.

**(d) Elution step**

The genomic DNA was recovered in the elution tube after adding 200  $\mu$ l of Tris-EDTA elution buffer to the column and centrifuging it for 1 min at 6500 rcf.

**2.5. Agarose Gel Electrophoresis**

To check the quality, DNA was run on 1% agarose gel. For 1% agarose gel (50 ml volume), 0.5 g of agarose and 5 ml of 10X TBE (0.025 M Borate, 0.89 M Tris, 0.032 M EDTA) were added in 45 ml of distilled water in a beaker. Now to make the agarose completely dissolved in the solution, the turbid agarose solution was placed in microwave oven for 1-2 minutes to get a clear solution. After that, add 0.6 ml of ethidium bromide dye and shake it well. Keep the spacer or comb in gel tank. Then slowly add the mixture add then cool it for 35-40 min for solidification. The combs were carefully removed when the gel had solidified, and the gel was then put in a tank with 1X TBE (running buffer). DNA was put into the gel's wells along with 4  $\mu$ l of loading dye (25% bromophenol blue and 40% sucrose). After loading, the gel tank was connected with power supply and was run at 120 volts for 20-30 minutes. The gel was then placed in the UV transilluminator (FluorChem FC3) digital camera EDAS 290 (Kodak, New York, USA) is used for image taken.

## 2.6 Homozygosity Mapping

In the current study homozygosity mapping of 3 skeletal dysplasia families (A, B, C) for the known loci was carried out by microsatellite markers. The physical distance of these known loci identified through UCSC genome browser and the genetic distance of the microsatellite markers flanking these loci was founded on the basis of this physical distance. To confirm the homo and heterozygosity of these microsatellite markers in affected and normal individuals, 5-10 microsatellite markers of different centimorgans (cM) in the vicinity of the particular locus were used.

## 2.7 Polymerase chain reaction (PCR)

The DNA dilutions were proceeded for amplification through polymerase chain reaction using specific STS markers. For preparation of PCR reaction mixture, 200 ml PCR tubes were used (Axygen, California, USA).

Table 2.2 PCR Reaction Mixture

Chemicals	Amounts
DNA	1 $\mu$ l
PCR buffer	2.5 $\mu$ l
Mg	2 $\mu$ l
DNTPs	0.5 $\mu$ l
Taq Polymerase	0.4 $\mu$ l
Primers (F and R)	0.4 $\mu$ l
PCR water	17.9 ml

The reaction mixture was vortexed using vertexer and then placed in T3 Thermocycler (Biometra, Gottingen, Germany). The standard PCR conditions were followed which are, Initial Denaturation of the genomic DNA at 96°C for 7-10 minutes which is then followed by amplification cycles (40). These amplification cycles consist of 3 repeating steps:

Denaturation of DNA at 96°C for 1 minute. Then Primer annealing with DNA (Temperature should be adjusted accordingly) for 1 minute. After annealing Renaturation of the DNA at 72°C for 1 minute. Final renaturation is carried out at 72°C for 10 minutes.



## 2.8 Polyacrylamide Gel electrophoresis (Vertical Gel)

On an 8% non-denaturing polyacrylamide gel, the microsatellite marker PCR products were resolved.

**Table 2.3 Composition of Polyacrylamide Gel**

Chemicals	Amounts
30% Acrylamide	14 ml
10X TBE	5 ml
10% APS	400 µl
TEMED	27 µl
Distilled water	Rise up to 50 ml

For 8% polyacrylamide gel (1 plate), 14 ml acrylamide solution (MERCK, Darmstadt, Germany) containing acrylamide and N, N, Methylene-bisacrylamide (BDH, Poole, England) added in 29:1, 5 ml 10X TBE (0.89 M Tris, 0.025 M Borate, 0.02 M EDTA), 10% APS 350 µl (Sigma-aldrich, St. Louis, MO, USA) were added in the measuring cylinder. distilled water were added to rise the volume upto 50ml (Tab 2.3). 27µl N,N,N,N Tetra methylethylene diamine (TEMED) (Sigma-aldrich, St.Louis, MO, USA) was added to catalyze the process. Gel loading plate was prepared by combining two plates. Space b/w two plates are 1.5 mm. After loading the gel, combs were inserted into the gel plate for creating wells to load DNA. The gel was then allowed to solidify

at 25°C for 30-45 min. Amplified product was mixed with 6 µl of tracking dye (sucrose (40%) and bromophenol blue (0.25%) solution) and then loaded in the gel. In apparatus (Whatman, Biometra, Gottingen, Germany) electrophoresis occurred at 147 volts and required two to three hrs. to complete. With ethidium bromide solution the gel is stained to make the DNA visible under ultra violet transilluminator (Biometra, Gottingen, Germany). Gel pictures were taken using digital camera EDAS 290 (Kodak, New York, USA).

## 2.9 Gene sequencing

After screening of linkage of markers to the respective loci, the linked gene/s were subjected to sanger sequences. Using online tools primer 3 (version 4), primers for all the exons of the linked gene/s were designed.

### 2.9.1 First Sequencing PCR

For the amplification of all the linked gene/s, The DNA dilutions were proceeded for amplification through polymerase chain reaction using Primers (table 2.2). For preparation of PCR reaction mixture, 200 µl PCR tubes were used (Axygen, California, USA).

The following chemicals are used. Take 1 µl of DNA, 1 µl of forward and 1 µl of reverse primer in PCR tube. Prepare master mix by taking 2.5 µl of PCR buffer, 2 µl of Mg, 0.5 µl of DNTPS and 0.3 µl of Taq polymerase. Then add 22 µl of master mix to each pcr tube and vortex the tube. The reaction mixture is placed in T3 Thermocycler (Biometra, Gottingen, Germany). The standard PCR conditions were followed which are;

Initial Denaturation of the genomic DNA at 96°C for 7-10 minutes which is then followed by amplification cycles (40). These amplification cycles consist of 3 repeating steps:

Denaturation of DNA at 96°C for 1 minute. Then Primer annealing with DNA (Temperature should be adjusted accordingly) for 1 minute. After annealing Renaturation of the DNA at 72°C for 1 minute.

Final renaturation is carried out at 72°C for 10 minutes. After PCR, the products were run on 2% agarose gel to check the specificity of the amplified products. The specific products were then purified via kit (Invitrogen, CA, USA).

#### 2.9.1.1 Purification of products of First sequencing PCR

After the confirmation of specific exonic amplification on 2% agarose gel, the specific products were then purified via kit (Fermentas, USA). The purification protocol is as follows:

- Add binding buffer at 1:3 in the amplified product and was properly mixed
- The mixture of PCR product and binding buffer was transferred to purification columns and was spun for 1 min at 13,000 rpm.
- After centrifugation discarded the liquid in collection tube.
- For the removal of unused primers, dNTPs, polymerase and buffer, 500 µl of wash buffer was added and then centrifugation at 13000 rpm for 1 minute and discard the flow through.
- an empty spin was given at 13000 rpm for 2 minutes.
- The column was transferred to new Eppendorf tube and 22µl of elution buffer was added.
- After incubation, again spin at 13000 rpm for 1 minutes to collect the purification product.

#### 2.10 Analysis of Sequenced data

Using Bio Edit alignment editor version 7.1.3.0 the sequenced data was analyzed by comparing chromatograms of exons of gene of affected individual with normal version of the corresponding gene to check nucleotide variation in the sequence of the exons. The sequence of the gene was downloaded from Ensemble Genome Browser database (<http://www.ensembl.org/index.html>). The variants found were then compared with the cDNA of the corresponding gene to check that the variants are pathogenic or not.

Table 2.4: List of the Microsatellite Markers of Family A

S. No	Gene/Locus	Cytogenic Location	Microsatellite Markers	Genetic location cM
01	GALNS	16q24.3	D16S3077	128.98
			D16S3063	129.12
			D16S3048	129.12
			D16S689	129.5
			D16S2621	131.01
			D16S3023	131.01
			D16S3026	132.01
02	NPR2	9P13.3	D16S3121	132.51
			D9S1878	58.75
			D9S1817	59
			D9S761	59.74
			D9S1794	60.25
			D9S50	60.81

			D9S1874	61.38
			D9S200	61.8

Table 2.5: List of the Microsatellite Markers of Family B

S. No	Gene/Locus	Cytogenetic Location	Microsatellite Marker	Genetic Location (cM)
03	<i>DLL3</i>	19q13.2	D19S1170	54.58
			D19S555	55.06
			D19S416	56.28
			D19S191	60.46
			D19S224	61.85
04	<i>MECP2</i>	15q26.1	D15S127	96.01
			D15S158	97.03
			D15S1004	106.17
			D15S531	106.17
05	<i>TBX6</i>	16p11.2	D16S3145	54.03
			D16S3120	55.25
			D16S3022	56.77
			D16S746	58.95

			D16S3105	59.06
--	--	--	----------	-------

Table 2.6: List of the Microsatellite Markers of Family C

S. No	Gene/Locus	Cytogenetic Location	Microsatellite Marker	Genetic Location
06	<i>HES7</i>	17p13.1	D17S578	18.59
			D17S960	19.66
			D17S1353	20
			D17S1812	20.5
			D17S1844	21.35
			D17S1791	23.59
07	<i>RIPPLY2</i>	6q14.12	D6S445	95.53
			D6S391	96.58

			D6S1609	96.66
			D16S1627	97.06
			D16S1644	98.97
08	LFNG	7p22.3	D7S616	4.79
			D7S2521	5.38
			DS7531	5.81
			D7S2424	5.83
			D7S3056	6.96

Table 2.7: Primers for *NPR2* Exons amplification

S. No	Primer Name	Primer Sequence	Ta	Product size (bp)
-------	-------------	-----------------	----	-------------------

1	NPR2-1F1	CTAGCCTACTCCTCCTCTTC	52.6	640
	NPR2-1R1	CATCCAGGTACAGCAAGGCA	62.2	
2	NPR2-1F2	CCAGAACACAACCTGAGCTA	56.5	684
	NPR2-1R2	CCACATACAGCTGCTCAATG	57.9	
3	NPR2-2F-6	GCTGAAGAGGGACATCCCAGTG	65.5	399
	NPR2-2R-6	CCTGCCTGGTTCCTAGGGTTTC	65.3	
4	NPR2-3F	CCAAGTTTCCCTGTCCTGCA	64	284
	NPR2-3R	CACAGCCAAGACTTGATGCT	63	

	NPR2-4F	CCAGAAGAGAGAATAGGTAG	48.3	
--	---------	----------------------	------	--



5	NPR2-4R	CGACTGAACCCTTGAAAGCT	59.5	622
6	NPR2-5F	GTAGGCATGAGTGAGTGGGA	58.7	619
	NPR2-5R	GCAGAAGCACAGTTAAGAGTG	55.5	
7	NPR2-6F	CACTCTTAAGTGTGCTTCTGC	55.5	323
	NPR2-6R	CCACATTATAGGGACCACCT	56.3	
8	NPR2-7F	CAGTTGCAGCTTCAGGAGCT	60.9	898
	NPR2-7R	CCACTACATAAGAGGACCTT	50.9	

	NPR2-8F	CATCCTTCCGCCTCCATGTT	64.5	
--	---------	----------------------	------	--

9	NPR2-8R	CCACTACATAAGAGGACCTT	50.9	544
10	NPR2-9F	CGGCAGGTTCTGTTTGA ACT	60.3	643
	NPR2-9R	CAGGACTTCAGAGGACTAGA	51.9	
11	NPR2-10F	GATCTGTAGACAGCTAGCCA	53.1	877
	NPR2-10R	GCACTAGGACTAATGAGTCT	48.4	
12	NPR2-11F	GTGGAGTGACAGTAATATAGG	48.9	553
	NPR2-11R	GCACTAGGACTAATGAGTCT	48.4	

## Chapter 03

### Results

### 3. RESULTS

#### 3.1 Families Descriptions

The current research was conducted on three families (A, B, and C) showing characteristic phenotypes of Acromesomelic dysplasia and spondylocostal dysostosis. These families were sampled from different areas of Pakistan. The clinical description and genetic analysis of these families are discussed below:

##### 3.1.1 Family A

Family A was sampled from the rural area of Multan, Pakistan. Affected members segregated dwarfism phenotypes in an autosomal recessive manner. Blood samples [5-10ml] were collected from two available affected (IV-2, IV-4) and one unaffected individual (III-4) for DNA extraction and further genetic analysis (Fig 3.1). Both affected individuals (IV-2) were born from two healthy Pakistani consanguineous parents manifested short stature (102cm and 100cm), arm spin, bowed forearm (radius looks shorter than ulna), short neck, pectus carinatum, pectus excavatum, kyphoscoliosis, brachydactyly in hands and feet, bowed leg bone, short and blunt nails, loose and redundant skin on hands.

##### 3.1.2 Family B

Family B was recruited from Murree, Pakistan. Pedigree analysis revealed an autosomal recessive inheritance pattern of the disorder. Blood samples from two affected [V-2, V-3] and four normal members were collected for genetic investigation (Fig 3.2). The affected individuals exhibited skeletal deformities including dwarfism, abnormality of chest bones, and extension of rib bones to the lower part of the abdomen (Fig 3.3).

##### 3.1.3 Family C

Family C was sampled from kund yaaro, Punjab, Pakistan. Pedigree analysis manifested autosomal recessive inheritance pattern of disease and exhibited three loops A, B, and C) Fig 3.4 Our study focused on loop C containing one affected and three normal individuals. The affected individual showed scoliosis, a short neck, short stature, asymmetrical body axis, rib anomalies such as pectus carinatum, and scapular dyskinesis due to which shoulder movement was restricted (Fig 3.5). Facial

abnormalities were also seen such as hypertelorism, widely spaced teeth, and high philtrum.

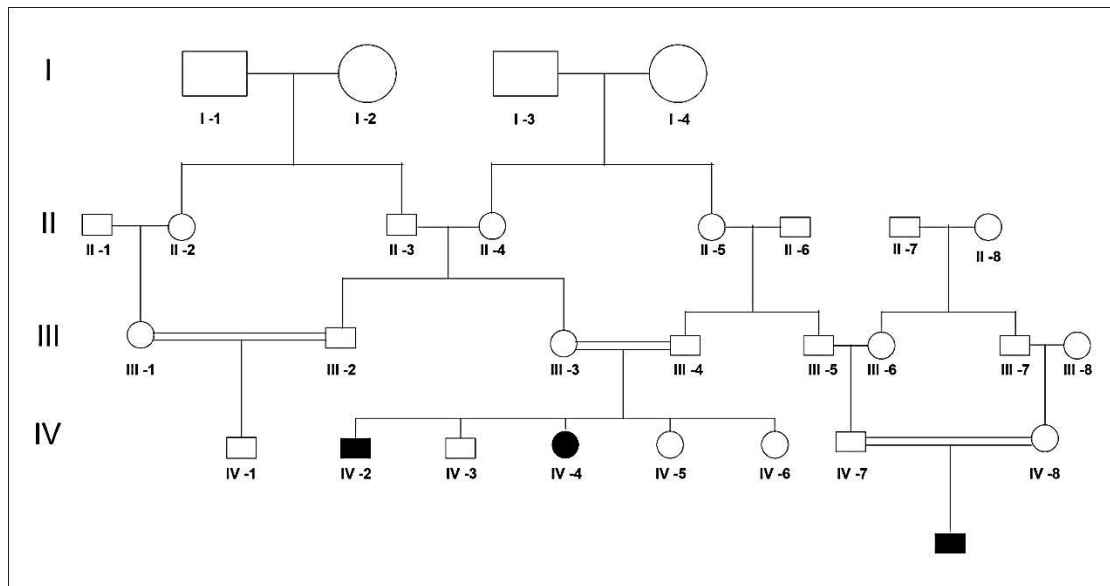
### 3.2 Mapping of Genes Involved in Hereditary Skeletal Disorders

Linkage analysis to known loci and genes for Acromesomelic dysplasia (*GDF5*, *NPR2*, *CDMP1*) in Family A and spondylocostal dystosis (*DLL3*, *TBX6*, *HES7*, *MESP2*, *LFNG*, and *RIPPLY2*) in Family B and C were carried out through highly polymorphic markers. Microsatellite markers were chosen from the gene flanking areas for genotyping. Microsatellite marker amplification was carried out using the common PCR procedure described in the technique (Tab 2.5) and the outcomes were examined on stained polyacrylamide gel (8% non-denaturing) using a UV Transilluminator.

In family A, the DNA of one affected and two normal members were tested for linkage analysis. Linkage analysis was performed using polymorphic microsatellite markers flanking *GALNS* (16q24.3) and *NPR2* (9p13.3) gene (Table 2.5). Linkage analysis revealed a homozygous region on chromosome 16q24.3 having *NPR2* gene (Fig 3.7). *NPR2* consists of 22 exons. In the current study, a total of 15 exons were amplified by using their specific primers. Purified products were then sent for Sanger sequencing. Analysis of the sequencing data did not reveal a pathogenic variant in 15 exons suggesting that the variant can be in the rest of the exons.

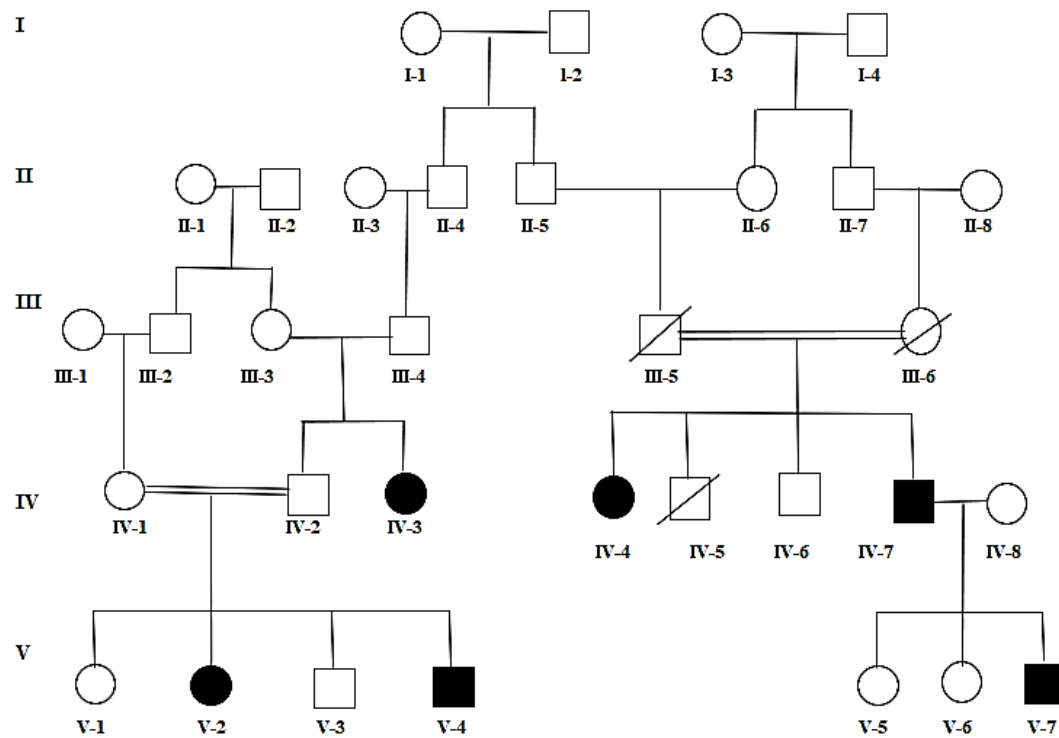
Family B and C manifested the classical features of spondylocostal dystosis. In family B DNA of two normal and two affected individuals while in family C three normal and one affected members was tested for linkage by typing microsatellites markers for respective candidate genes including *DLL3* (19q3.2), *HES7* (17p13.1), *TBX6* (16p11.2), *MESP2* (15q26.1), *LFNG* (7p22.3). *RIPPLY2* (6q14.2: Table 2.5) The genotyping of the markers failed to show any homozygous pattern for alleles, showing that the family was not linked to any of these selected six genes (Fig 3.8-3.18).

### 3.1.1.1 Pedigree of Family A

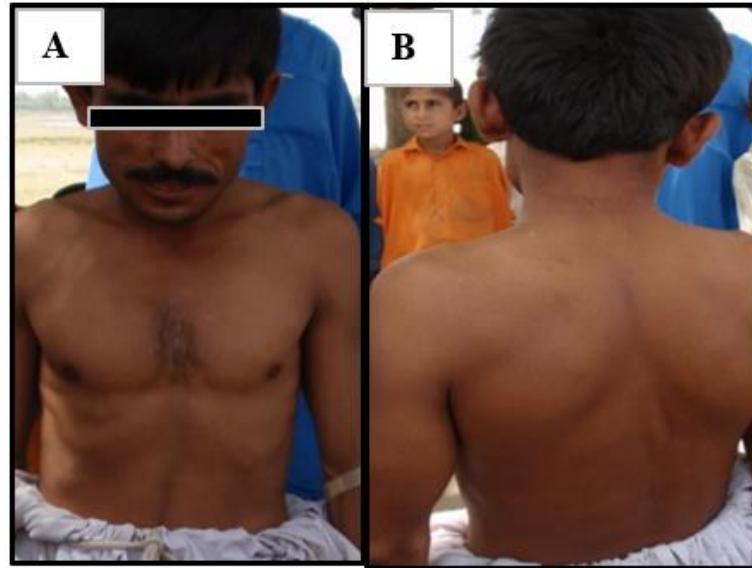


**Figure 3.1:** Pedigree of family A having an autosomal recessive inheritance pattern. Affected members were represented by filled black circles and squares while empty circles and squares were used for normal members. Cousin marriage between individuals was shown by a double line. Generation and family members were represented by the Roman and Arabic numerals respectively. III-4, IV-2, and IV-4 members were recruited for the current study.

## 3.1.2.1 Pedigree of Family B

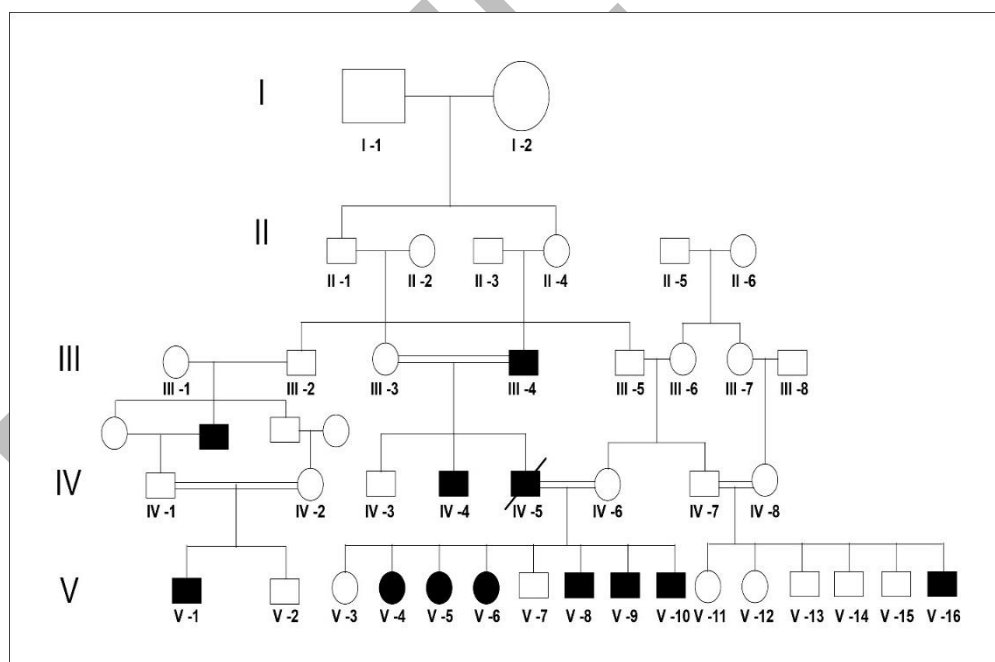


**Figure 3.2:** Pedigree of family B having an autosomal recessive inheritance pattern. Affected members were represented by filled black circles and squares while empty circles and squares were used for normal members. Cousin marriage between individuals was shown by a double line. Generation and family members were represented by the Roman and Arabic numerals respectively. IV-1, V-1, V-2, and IV-4 members were recruited for the current study.



**Figure 3.3:** A, B: Affected member of family B showing abnormality of chest bone, scapula deformity and asymmetric body stature.

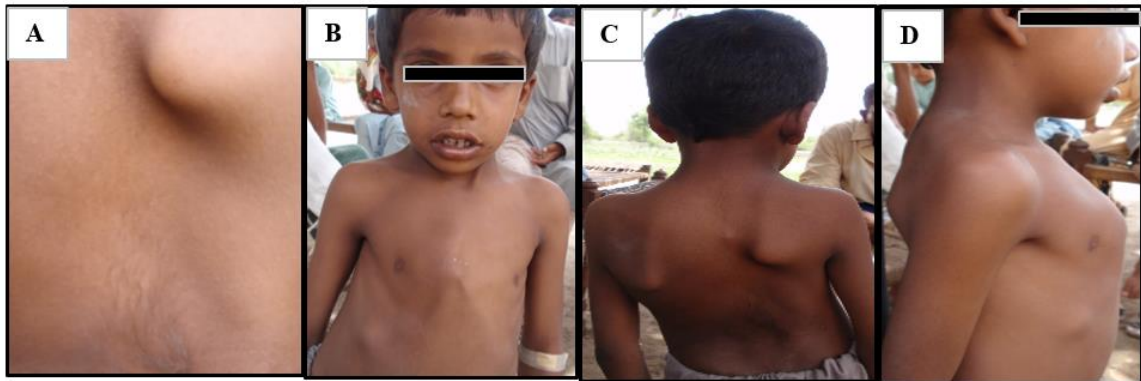
### 3.1.3.1 Pedigree of Family C



**Figure 3.4:** Pedigree of family C having an autosomal recessive inheritance pattern. Affected members were represented by filled black circles and squares while empty circles and squares were used for normal members. Cousin marriage between individuals was shown by a double line. Generation and family members were



represented by the Roman and Arabic numerals respectively. IV-7, IV-8, V-15 and V-16 members were subjected for the current study.



**Figure 3.5:** A, C: Affected individual in family C exhibiting pectus carinatum and showing scapular dyskinesis (B, D).

### 3.3 Mapping of Genes Involved in Hereditary Skeletal Disorders

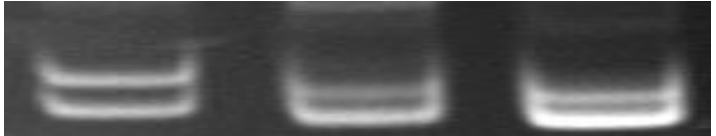
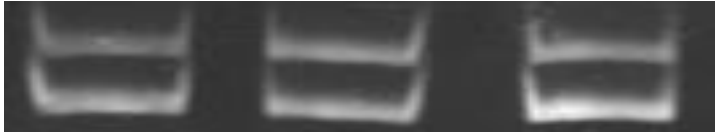

Linkage analysis to known loci and genes for Acromesomelic dysplasia (*GDF5*, *NPR2*, *CDMP1*) in Family A and spondylocostal dystosis (*DLL3*, *TBX6*, *HES7*, *MESP2*, *LFNG*, and *RIPPLY2*) in Family B and C was carried out through highly polymorphic markers. Microsatellite markers were chosen from the gene flanking areas for genotyping. Microsatellite marker amplification was carried out using the common PCR procedure described in the technique (Tab 2.5) and the outcomes were examined on stained polyacrylamide gel (8% non-denaturing) using a UV Transilluminator.

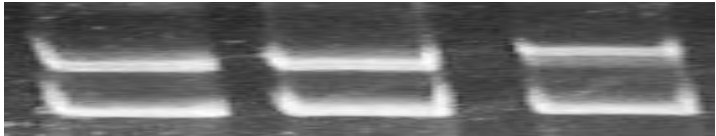
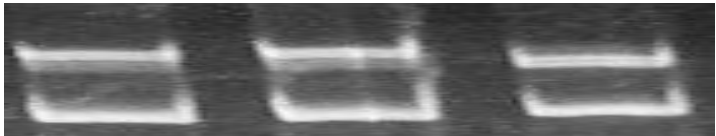

In family A, DNA of one affected and two normal members was tested for linkage analysis. Linkage analysis was performed using polymorphic microsatellite markers flanking *GALNS* (16q24.3) and *NPR2* (9p13.3) gene (Table 2.5). Linkage analysis revealed homozygous region on chromosome 16q24.3 having *NPR2* gene (Fig 3.7). *NPR2* consists of 22 exons. In the current study a total of 15 exons were amplified by using their specific primers. Purified products were then sent for Sanger sequencing. Analysis of the sequencing data did not reveal pathogenic variant in 15 exons suggesting that variant can be in the rest of the exons.

Family B and C manifested the classical features of spondylocostal dystosis. In family B DNA of two normal and two affected individuals while in family C three normal and one affected members was tested for linkage by typing microsatellites markers for respective candidate genes including *DLL3* (19q3.2), *HES7* (17p13.1), *TBX6* (16p11.2), *MESP2* (15q26.1), *LFNG* (7p22.3). *RIPPLY2* (6q14.2: Table 2.5) The genotyping of the markers failed to show any homozygous pattern for alleles, showing that the family was not linked to any of these selected six genes (Fig 3.8-3.18).

### 3.1.1.2. Homozygosity Mapping of Family A

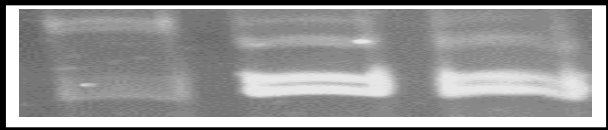
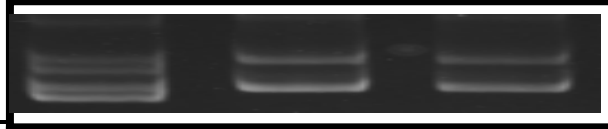
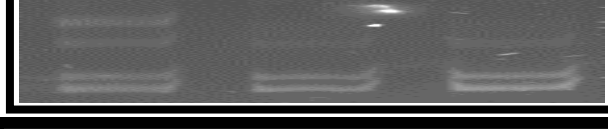
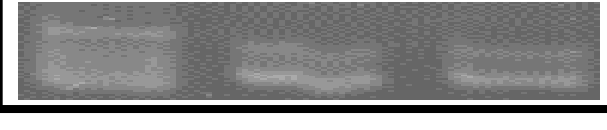
#### *GALNS*

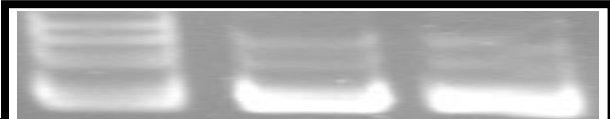
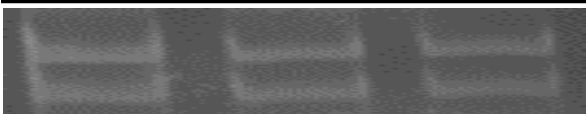
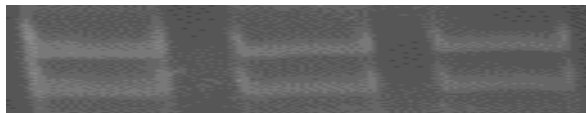
S. No	Markers ID	Cytogenic position (cM)	1 Normal	2 Affected	3 Affected
1	D16S689	129.5			
2	D16S2621	131.01			
2	D16S3023	131.01			

3	D16S3121	132.5	
4	D16S3063	129.12	
5	D16S3077	128.98	

**Figure 3.6:** Results of the *GALNS* flanking microsatellite markers in family A.

#### *NPR2*


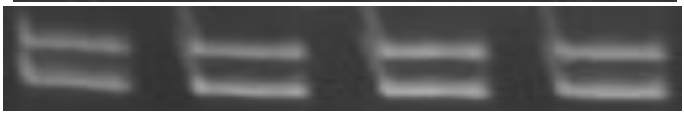

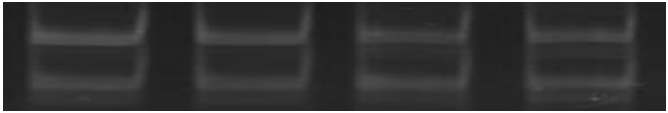
S. No	Markers ID	Cytogenic position (cM)	1 Normal	2 Affected	3 Affected
1	D9S1878 (linked)	58.75			
2	D9S1817	59			
3	D9S1874(linked)	61.38			
4	D9S2007(linked)	61.8			

5	D9S50 (Linked)	60.51	
6	D9S761	69.74	
7	D9S1794	60.25	

**Figure 3.7:** Results of the *NPR2* flanking microsatellite markers in family A.

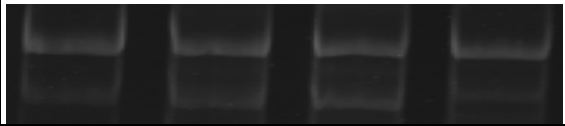




### 3.1.2.2 Homozygosity Mapping of Family B

#### *DLL3*

S. No	Markers ID	Cytogenic position (cM)	1 Normal	2 Normal	3 Affected	4 Affected
1	D19S1170	54.58				
2	D19S555	55.06				
3	D19S416	56.28				
4	D19S220	62.62				

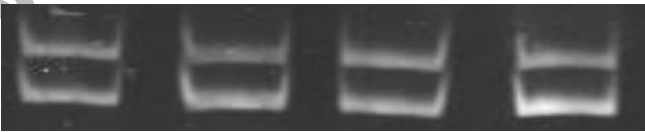
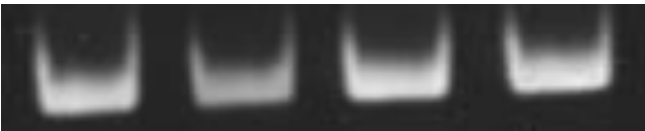

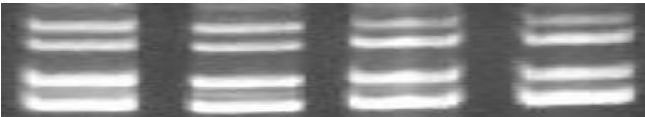
**Figure 3.8:** Results of the *DLL* flanking microsatellite markers in family B.

*TBX6*

S. No	Markers ID	Cytogenic position (cM)	1 Normal	2 Normal	3 Affected	4 Affected
1	D16S3145	54.03				
2	D16S3022	56.77				
3	D16S746	58.95				
4	D16S3120	55.25				
5	D16S3105	59.0^				

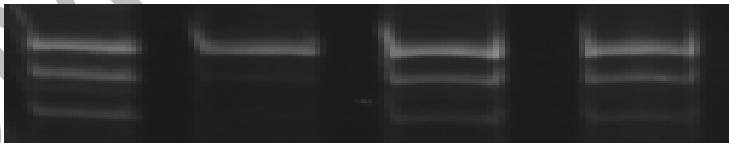
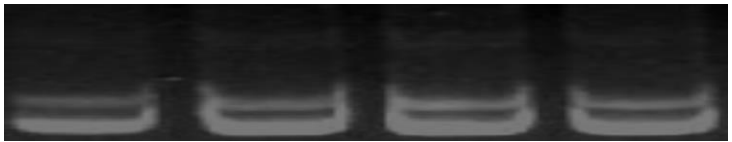
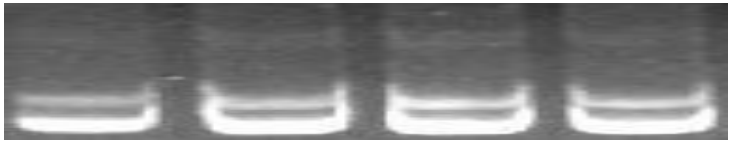
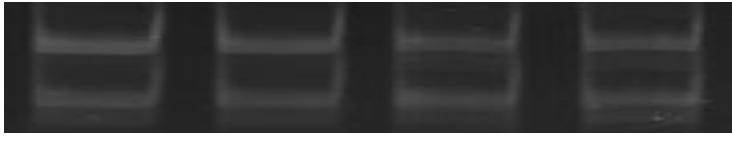
**Figure 3.9:** Results of the *TBX6* flanking microsatellite markers in family B.

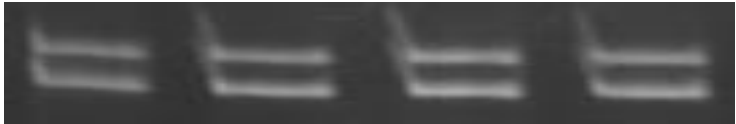
*HES7*

S. No	Markers ID	Cytogenic position (cM)	1 Normal	2 Normal	3 Affected	4 Affected
1	D17S960	19.66				
2	D17S578	18.59				
3	D17S1812	20.5				
4	D17S1844	21.35				

**Figure 3.10:** Results of the *HES7* flanking microsatellite markers in family B.

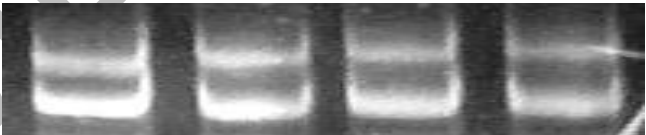
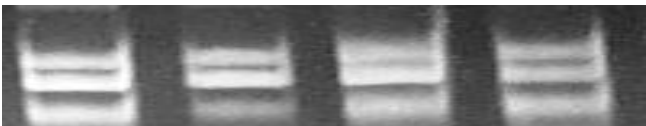
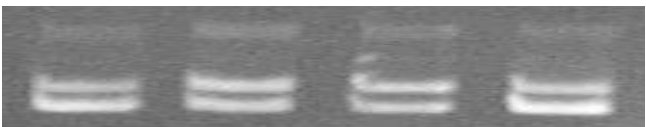

**RIPPLY2**

S. No	Markers ID	Cytogenic position (cM)	1 Normal	2 Normal	3 Affected	4 Affected
1	D6S391	96.58				
2	D6S1627	97.06				
3	D6S445	95.53				
4	D6S1644	98.97				

5	D6S169	96.66	
---	--------	-------	--

**Figure 3.11:** Results of the *RIPPLY2* flanking microsatellite markers in family B.

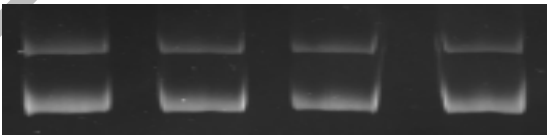
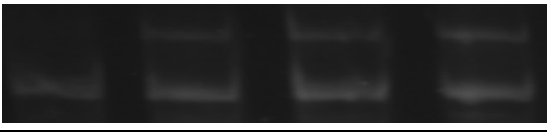
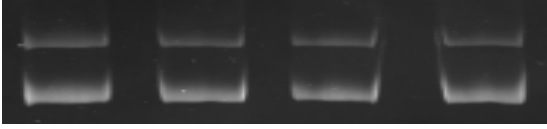
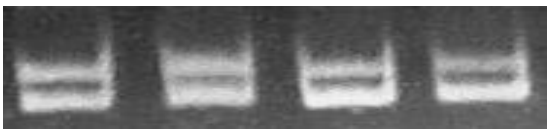
### *LFNG*

S. No	Markers ID	Cytogenic position (cM)	1 Normal	2 Normal	3 Affected	4 Affected
1	D7S616	4.97				
2	D7S531	5.81				
3	D7S2424	5.83				
4	D7S2521	5.38				

**Figure 3.12:** Results of the *LFNG* flanking microsatellite markers in family B.



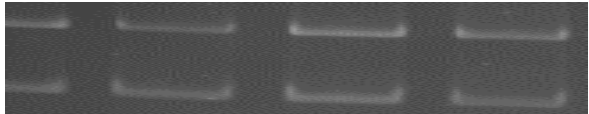


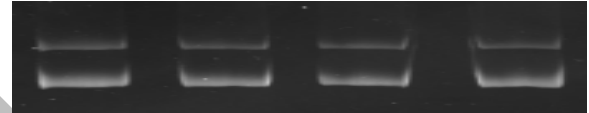
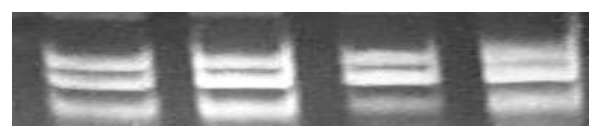
*MECP2*

S. No	Markers ID	Cytogenic position (cM)	1 Normal	2 Normal	3 Affected	4 Affected
1	D15S1004	106.17				
2	D15S127	96.01				
3	D15S531	106.17				
4	D15S158	97.03				

**Figure 3.13:** Results of the *MECP2* flanking microsatellite markers in family B.

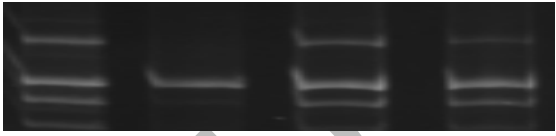
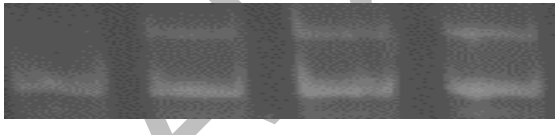
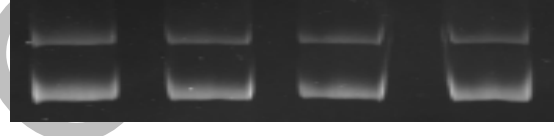
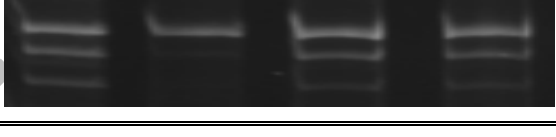
## 3.1.3.2 Homozygosity Mapping of Family C

*DLL3*

S. No	Markers ID	Cytogenic position (cM)	1 Normal	2 Normal	3 Normal	4 Affected
1	D19S1170	54.58				
2	D19S555	55.06				
3	D19S416	56.28				
4	D19S220	62.62				
5	D19S191	60.46				

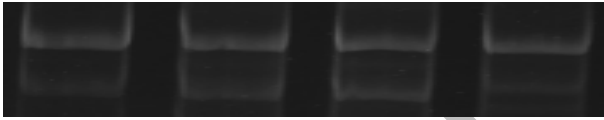


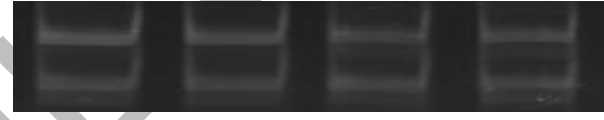
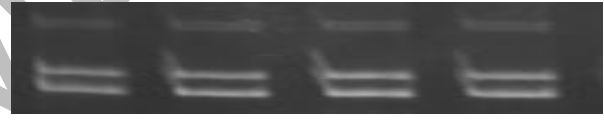
**Figure 3.14:** Results of the *DLL3* flanking microsatellite markers in family C.

**MECP2**

S. No	Markers ID	Cytogenic position (cM)	1 Normal	2 Normal	3 Normal	4 Affected
1	D15S1004	106.17				
2	D15S127	96.01				
3	D15S531	106.17				
4	D15S158	97.03				

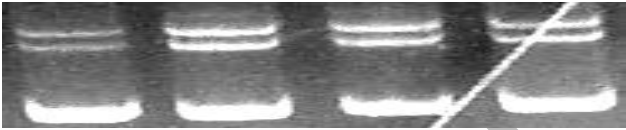
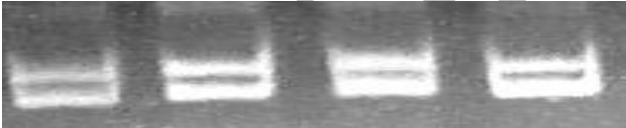
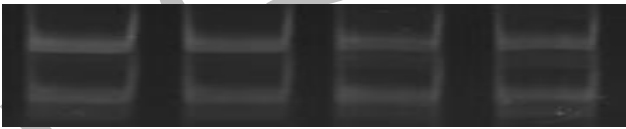

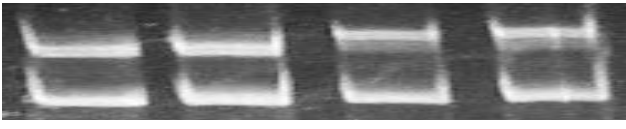
**Figure 3.15:** Results of the *MECP2* flanking microsatellite markers in family C.

***TBX6***

S. No	Markers ID	Cytogenic position (cM)	1 Normal	2 Normal	3 Normal	4 Affected
1	D16S3145	54.03				
2	D16S3022	56.77				
3	D16S746	58.95				
5	D16S3120	55.25				
6	D16S3105	59.0				

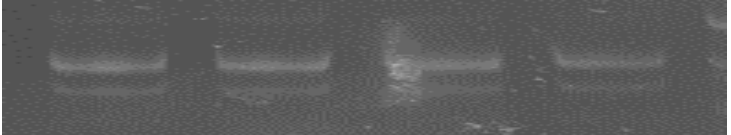
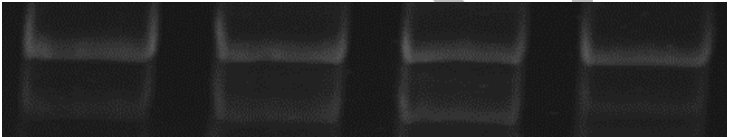
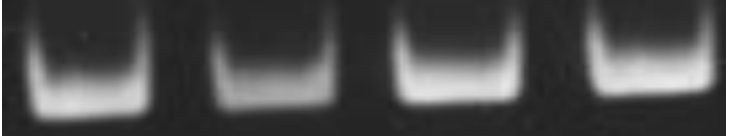
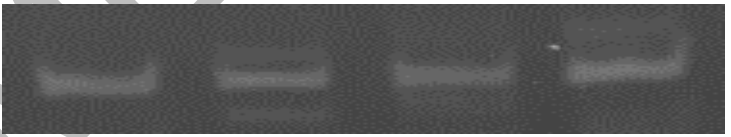
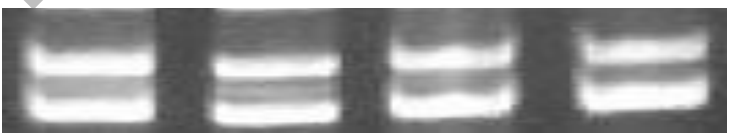
**Figure 3.16:** Results of the *TBX6* flanking microsatellite markers in family C.

*HES7*

S. No	Markers ID	Cytogenic position (cM)	1 Normal	2 Normal	3 Normal	4 Affected
1	D17S960	19.66				
2	D17S578	18.59				
3	D17S1812	20.5				
4	D17S1844	21.35				
5	D17S1353	20				

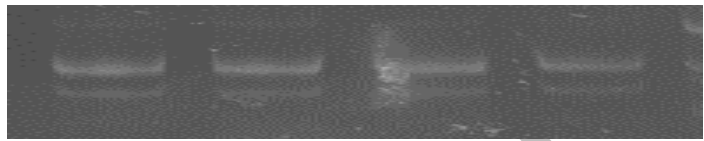

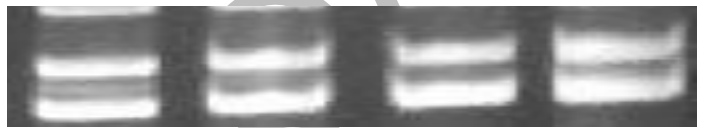
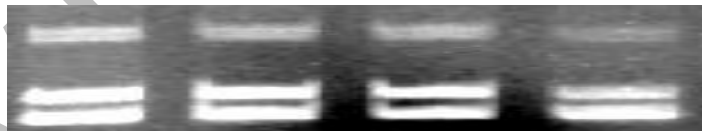
**Figure 3.17:** Results of the *HES7* flanking microsatellite markers in family C.

**RIPPLY2**

S. No	Markers ID	Cytogenic position (cM)	1 Normal	2 Normal	3 Normal	4 Affected
1	D6S391	96.58				
2	D6S1627	97.06				
3	D6S445	95.53				
4	D6S1644	98.97				
5	D6S169	96.66				

**Figure 3.18:** Results of the *RIPPLY2* flanking microsatellite markers in family C.

*LFNG*

S. No	Markers ID	Cytogenic position (cM)	1 Normal	2 Normal	3 Normal	4 Affected
1	D7S616	4.97				
2	D7S531	5.81				
3	D7S2424	5.83				
4	D7S2521	5.38				

**Figure 3.19:** Results of the *LFNG* flanking microsatellite markers in family C.

DRSML QAU



# **Chapter 04**

## **Discussion**

## 4. Discussion

Skeleton is one of the crucial organ systems in the human body. Skeleton provide support, protection and perform other function like help in movement etc. The development of the skeleton is a complex process that involves several genes along with morphological processes such as patterning, condensation, and achievement of a final form. Various skeletal abnormalities, commonly known as skeletal disorders, caused by mutations in genes that are responsible for the embryonic phases of skeletal creation and/or post-developmental maintenance. There are now 461 identified skeletal disorders that can cause a variety of skeletal deformities. (Warman *et al.*, 2010; Mortier *et al.*, 2019). Genetic mutations are the root cause of skeletal abnormalities. Hereditary skeletal conditions can be inherited as X-linked, recessive conditions or autosomal dominant (Warman *et al.*, 2010; Mortier *et al.*, 2019).

The risk of genetic disorder rises with cousin marriages. According to the theory that a certain region of the siblings' genomes from cousin marriages would be homozygous because of identity through descent. It is anticipated that one out of sixteenth of the genomes of children from first cousin marriages will be homozygous. With the exception of a certain sickness locus that all sick siblings share. The remaining homozygosity among the many progenies of these cousin marriages is random. (Sheffield *et al.*, 1995).

In the current study, three families (A, B, and C) with skeletal disorders were characterized clinically and genetically. These families belonged to different cities of Pakistan. Family A belong to Multan, Punjab and show phenotypes of Acromesomelic dysplasia. Family B belong to Muree, Punjab and show clinical features of Spondylocostal dysostosis. While, Family C belong to Kund yaroo, Punjab and show clinical features of Spondylocostal dysostosis.

Family A was represented with three members (III-2, IV-1, IV-3) with two affected members (IV-1, IV-3) showing short stature (102cm and 100cm), arm spin, bowed forearm (radius looks shorter than ulna), short neck, pectus cranatum, pectus excavatum, kyphoscoliosis, bradydactyly in hands and feet, bowed leg bone, blunt and short nails, redundant and loose skin on hands and one normal member (III-2). This

disorder was inherited in an autosomal recessive pattern and the affected member was a result of a consanguineous marriage.

Genotyping showed that the family was linked with the *NPR2* gene on chromosome 9p13.3. Sanger Sequencing was then carried out for *NPR2* Gene. 14 out of 21 Exons were sequenced and showed no mutation which suggest that mutation is present in the rest of the exons.

On chromosome 9p13.3, the AMDM-causing gene *NPR2* has 22 exons spread over 16.5 kb. The gene produces a protein of 1047 amino acids. (Kant *et al.*, 1998). C-type natriuretic peptide (CNP) is the product of *NPR2*. The modular structure of NPR-B, a homodimeric transmembrane protein, includes an extracellular domain that binds ligands, , an intracellular kinase homology domain, a trans-membrane unit and a carboxyl-terminal guanylyl cyclase domain. (Olney *et al.*, 2006). NPR-B a receptor of CNP is considered as crucial longitudinal growth regulators that plays a role in endochondral ossification. (Umair *et al.*, 2015). CNP has remarkable expression in the hypertrophic zone of the growth plate, where it promotes chondrocyte differentiation and proliferation in an paracrine/autocrine way to promote cartilage formation. (Pejchalova *et al.*, 2007). When CNP binds to NPR-B, cyclic GMP (cGMP) accumulates intracellularly, activating downstream signaling molecules such cyclic nucleotide-regulated ion channels (cGICs), cyclic GMP-regulated phosphodiesterases (PDEs), and cGMP-dependent protein kinases I and II (cGKI and cGKII) (Olney, 2006; Pejchalova *et al.*, 2007). Till now cGKII is necessary for CNP-mediated endochondral ossification (Miyazawa *et al.*, 2002). Through the MAPK signaling route, CNP activates the FGFR3 pathway, which increases chondrocyte proliferation and differentiation and encourages the creation of cartilage matrix. (Vasques *et al.*, 2014). Disruption in the CNP/NPR-B signaling pathway will lead to abnormal differentiation, proliferation and homeostasis of osteoblast and osteoclasts which in turn leads to skeletal deformities (T Langenickel *et al.*, 2004).

Family B was represented with four members (two normal and two affected). The affected individuals exhibited skeletal deformities included dwarfism, abnormality of chest bones, and extension of rib bones to the lower part of the abdomen These anomalies are inherited in an autosomal recessive manner. The features of the affected members were searched in OMIM which revealed the involvement of six candidate

genes (*DLL3*, *HES7*, *TBX6*, *MESP2*, *LFNG*, *RIPPLY2*) in causing the disorders. For genotyping, polymorphic microsatellite markers flanking these candidate genes were used. Analysis of the results failed to show any homozygous pattern for alleles, showing no linkage to any of these selected six genes. Therefore, it is highly likely that a novel gene is involved in causing the disorder in the family.

Family C was represented with four members (three normal and one affected) and affected members showed multiple skeletal abnormalities including scoliosis, short neck, short stature, asymmetrical body axis, rib anomalies such as pectus carinatum and scapular dyskinesia due to which shoulder movement was restricted (Fig 3.5). Facial abnormalities were also seen such as hypertelorism, widely spaced teeth and high philtrum. These anomalies are inherited in an autosomal recessive manner. The features of the affected members were searched in OMIM which revealed the involvement of six candidate genes (*DLL3*, *HES7*, *TBX6*, *MESP2*, *LFNG*, *RIPPLY2*) in causing the disorders. For genotyping, polymorphic microsatellite markers flanking these candidate genes were used. Analysis of the results failed to show any homozygous pattern for alleles, showing that the family was not linked to any of these selected six genes. Therefore, it is highly likely that a novel gene is involved in causing the disorder in the family. For the identification of the novel gene, the exome sequencing technique will be used.

In conclusion, we could not identify the causative variant in the sequenced exons of *NPR2* gene which suggests the presence of causative variants in remaining exons in family A. The family B and C did not establish any linkage to the known genes underlying the phenotypes of these disorders; therefore, we presume the involvement of a novel gene/s. The disorders not resolved by traditional method of linkage analysis are suggested to be proceeded for exome analysis for comprehensive genetic analysis.

## **Chapter 05**

## **References**

## 5. References

- Ahmad, S., Ali, M. Z., Muzammal, M., Mir, F. A., & Khan, M. A. (2022). The molecular genetics of human appendicular skeleton. *Molecular Genetics and Genomics*, 1-20.
- Baehner F, Schmiedeskamp C, Krummenauer F, Miebach E, Bajbouj M, Whybra C, Beck M (2005). Cumulative incidence rates of the mucopolysaccharidoses in Germany. *J Inher Metab Dis* 28:1011-1017.
- Beine, O., Bolland, J., Verloes, A., Lebrun, F. R., Khamis, J., & Ch, M. (2004). Spondylocostal dysostosis: a rare genetic disease. *Revue Medicale de Liege*, 59(9), 513-516.
- Bonafe, L., Cormier-Daire, V., Hall, C., Lachman, R., Mortier, G., Mundlos, S., ... & Unger, S. (2015). Nosology and classification of genetic skeletal disorders: 2015 revision. *American journal of medical genetics Part A*, 167(12), 2869-2892.
- Brailsford JF. Chondro-osteo-dystrophy: Roentgenographic & clinical features of a child with dislocation of vertebrae. *The American Journal of Surgery*. 1929 Sep 1;7(3):404-10.
- Brennan A, & Kesavan, A. (2017). Novel heterozygous mutations in JAG1 and NOTCH2 genes in a neonatal patient with Alagille syndrome. *Case Reports in Pediatrics*, 2017.
- Bulman, M. P., Kusumi, K., Frayling, T. M., McKeown, C., Garrett, C., Lander, E. S., ... & Turnpenny, P. D. (2000). Mutations in the human delta homologue, *DLL3*, cause axial skeletal defects in spondylocostal dysostosis. *Nature genetics*, 24(4), 438-44
- Cadaoas J, Boyle G, Jungles S, Cullen S, Vellard M, Grubb JH, Jurecka A, Sly W, Kakkis (2020). Vestronidase alfa: Recombinant human  $\beta$ -glucuronidase as an enzyme replacement therapy for MPS VII. *Mol Genet Metab* 13:65-76.
- Cheema HA, Malik HS, Hashmi MA, Fayyaz Z, Mushtaq I, Shahzadi N (2017). Mucopolysaccharidoses—clinical spectrum and frequency of different types. *J Coll Physicians Surg Pak* 27:80-83.

- Clarke, B. (2008). Normal bone anatomy and physiology. *Clinical journal of the American Society of Nephrology*, 3(Supplement 3), S131-S139.
- Clarke, L. A., & Hollak, C. E. (2015). The clinical spectrum and pathophysiology of skeletal complications in lysosomal storage disorders. *Best practice & Research clinical endocrinology & Metabolism*, 29(2), 219-235.
- De Baat, P., Heijboer, M. P., & De Baat, C. (2005). Development, physiology, and cell activity of bone. *Nederlands tijdschrift voor tandheelkunde*, 112(7), 258-263.
- Fedele AO (2015). Sanfilippo syndrome: causes, consequences, and treatments. *Appl Clin Genet* 8:269.
- Fesslova V, Corti P, Sersale G, Rovelli A, Russo P, Mannarino S, Parini R (2009). The natural course and the impact of therapies of cardiac involvement in the mucopolysaccharidoses. *Cardiol Young* 19:170-178.
- Florencio-Silva, R., Sasso, G. R. D. S., Sasso-Cerri, E., Simões, M. J., & Cerri, P. S. (2015). Biology of bone tissue: structure, function, and factors that influence bone cells. *BioMed research international*, 2015.
- Fukuda S, Tomatsu S, Masuno M, Ogawa T, Yamagishi A, Maruf Rezvi GM, Orii T (1996). Mucopolysaccharidosis IVA: submicroscopic deletion of 16q24. 3 and a novel R386C mutation of N-acetylgalactosamine-6-sulfate sulfatase gene in a classical Morquio disease. *Hum Mutat* 7:123-134.
- Geister, K. A., & Camper, S. A. (2015). Advances in skeletal dysplasia genetics. *Annual Review of Genomics and Human Genetics*, 16, 199.
- Guasto, A., & Cormier-Daire, V. (2021). Signaling pathways in bone development and their related skeletal dysplasia. *International Journal of Molecular Sciences*, 22(9), 4321.
- Hall, B. K. (2005). *Bones and cartilage: developmental and evolutionary skeletal biology*. Elsevier.
- Hurst, J. A., Firth, H. V., & Smithson, S. (2005, June). Skeletal dysplasias. In *Seminars in Fetal and Neonatal Medicine* (Vol. 10, No. 3, pp. 233-241). WB Saunders.

involved in osteogenesis and their application for bone regenerative medicine. *Tissue Engineering Part B: Reviews*, 21(1), 75-87.

Jakkula, E., Mäkitie, O., Czarny-Ratajczak, M., Jackson, G. C., Damignani, R., Susic, M., ... & Ala-Kokko, L. (2005). Mutations in the known genes are not the major cause of MED; distinctive phenotypic entities among patients with no identified mutations. *European journal of human genetics*, 13(3), 292-301.

Kamath, B. M., Baker, A., Houwen, R., Todorova, L., & Kerkar, N. (2018). Systematic review: the epidemiology, natural history, and burden of Alagille syndrome. *Journal of pediatric gastroenterology and nutrition*, 67(2), 148.

Kant, S. G., Polinkovsky, A., Mundlos, S., Zabel, B., Thomeer, R. T., Zonderland, H. M., ... & Warman, M. L. (1998). Acromesomelic dysplasia Maroteaux type maps to human chromosome 9. *The American Journal of Human Genetics*, 63(1), 155-162.

Khan SA, Peracha H, Ballhausen D, Wiesbauer A, Rohrbach M, Gautschi M, Tomatsu S (2017). Epidemiology of mucopolysaccharidoses. *Mol Genet Metab* 121:227-240.

Khan, S., Basit, S., Khan, M. A., Muhammad, N., & Ahmad, W. (2016). Genetics of human isolated acromesomelic dysplasia. *European Journal of Medical Genetics*, 59(4), 198-203.

Kini, U., & Nandeesh, B. N. (2012). Physiology of bone formation, remodeling, and metabolism. In *Radionuclide and hybrid bone imaging* (pp. 29-57). Springer, Berlin, Heidelberg.

Kornak, U., & Mundlos, S. (2003). Genetic disorders of the skeleton: a developmental approach. *The American Journal of Human Genetics*, 73(3), 447-474.

Linker A, Meyer K, Weissmann B (1995). Enzymatic formation of monosaccharides from hyaluronate. *J Biol Chem* 213:237-248.

Marín-Llera, J. C., Garcíadiego-Cázares, D., & Chimal-Monroy, J. (2019). Understanding the cellular and molecular mechanisms that control early cell fate decisions during appendicular skeletogenesis. *Frontiers in Genetics*, 10, 977.



- Martinez-Garcia, M., Garcia-Canto, E., Fenollar-Cortes, M., Aytes, A. P., & Trujillo-Tiebas, M. J. (2016). Characterization of an acromesomelic dysplasia, Grebe type case: novel mutation affecting the recognition motif at the processing site of *GDF5*. *Journal of bone and mineral metabolism*, 34(5), 599-603.
- Marzin, P., & Cormier-Daire, V. (2020). New perspectives on the treatment of skeletal dysplasia. *Therapeutic advances in endocrinology and metabolism*, 11, 2042018820904016.
- Miyazawa, K., Shinozaki, M., Hara, T., Furuya, T., & Miyazono, K. (2002). Two major Smad pathways in TGF- $\beta$  superfamily signalling. *Genes to Cells*, 7(12), 1191-1204.
- Montaño AM, Lock Hock N, Steiner RD, Graham BH, Szlago M, Greenstein R, Pineda M, Gonzalez-Meneses A, Çoker M, Bartholomew D, Sands MS (2016). Clinical course of sly syndrome (mucopolysaccharidosis type VII). *J Med Genet* 53:403-418.
- Morquio L. Sur une forme de dystrophie osseuse familiale. *Bull Soc Pediatr Paris*. 1929; 27:145-52.
- Mortier, G. R. (2001). The diagnosis of skeletal dysplasias: a multidisciplinary approach. *European journal of radiology*, 40(3), 161-167.
- Mortier, G. R., Cohn, D. H., Cormier-Daire, V., Hall, C., Krakow, D., Mundlos, S., ... & Warman, M. L. (2019). Nosology and classification of genetic skeletal disorders: 2019 revision. *American Journal of Medical Genetics Part A*, 179(12), 2393-2419.
- Mortier, G. R., Cohn, D. H., Cormier-Daire, V., Hall, C., Krakow, D., Mundlos, S., ... & Warman, M. L. (2019). Nosology and classification of genetic skeletal disorders: 2019 revision. *American Journal of Medical Genetics Part A*, 179(12), 2393-2419.
- Muenzer J (2004). The mucopolysaccharidoses: a heterogeneous group of disorders with variable pediatric presentations. *J Pediatr* 144: S27-S34.
- Nakashima Y, Tomatsu S, Hori T, Fukuda S, Sukegawa K, Kondo N, Orii T (1994). Mucopolysaccharidosis IV A: molecular cloning of the human N-acetylgalactosamine-6-sulfatase gene (GALNS) and analysis of the 5'-flanking region. *Genomics* 20:99-104.

- Nelson J, Crowhurst J, Carey B, Greed L (2003). Incidence of the mucopolysaccharidoses in Western Australia. *Am J Med Genet Part A* 123:310-313.
- Neufeld EF (2001). The mucopolysaccharidoses. *Metabol Molec Bas Inherit Dis* 3421-3452.
- Neufeld EF (2001). The mucopolysaccharidoses. *Metabol Molec Bas Inherit Dis* 3421-3452.
- Olney, R. C., Bükülmez, H., Bartels, C. F., Prickett, T. C., Espiner, E. A., Potter, L. R., & Warman, M. L. (2006). Heterozygous mutations in natriuretic peptide receptor-B (*NPR2*) are associated with short stature. *The Journal of Clinical Endocrinology & Metabolism*, 91(4), 1229-1232.
- Pejchalova, K., Krejci, P., & Wilcox, W. R. (2007). C-natriuretic peptide: an important regulator of cartilage. *Molecular genetics and metabolism*, 92(3), 210-215.
- Pingault, V., Ente, D., Dastot-Le Moal, F., Goossens, M., Marlin, S., & Bondurand, N. (2010). Review and update of mutations causing Waardenburg syndrome. *Human mutation*, 31(4), 391-406.
- Rimoin, D. L., Cohn, D., Krakow, D., Wilcox, W., Lachman, R. S., & Alanay, Y. (2007). The skeletal dysplasias: clinical-molecular correlations. *Annals of the New York Academy of Sciences*, 1117(1), 302-309.
- Sambrook, J., Fritsch, E. F., & Maniatis, T. (1989). *Molecular cloning: a laboratory manual* (No. Ed. 2). Cold spring harbor laboratory press.
- Santamaria R, Blanco M, Chabas A, Grinberg D, Vilageliu L (2007). Identification of 14 novel *GLB1* mutations, including five deletions, in 19 patients with GM1 gangliosidosis from South America. *Clin Genet* 71:273-279.
- Savarirayan, R., & Rimoin, D. L. (2002). The skeletal dysplasias. Best practice & research *Clinical endocrinology & metabolism*, 16(3), 547-560.
- Schramm, T., Gloning, K. P., Minderer, S., Daumer-Haas, C., Hörtnagel, K., Nerlich, A., & Tutschek, B. (2009). Prenatal sonographic diagnosis of skeletal dysplasias.

Ultrasound in Obstetrics and Gynecology: The Official Journal of the International Society of Ultrasound in Obstetrics and Gynecology, 34(2), 160-170.

Sheffield, V. C., Nishimura, D. Y., & Stone, E. M. (1995). Novel approaches to linkage mapping. *Current opinion in genetics & development*, 5(3), 335-341.

Sohn YB, Park HD, Park SW, Kim SH., Cho SY, Ko AR, Jin DK (2012). A Korean patient with Morquio B disease with a novel c. 13\_14insA mutation in the GLB1 gene. *Ann Clin Lab Sci* 42:89-93.

Sparrow, D. B., Guillén-Navarro, E., Fatkin, D., & Dunwoodie, S. L. (2008). Mutation of Hairy-and-Enhancer-of-Split-7 in humans causes spondylocostal dysostosis. *Human molecular genetics*, 17(23), 3761-3766.

Stapleton M, Kubaski F, Mason RW, Yabe H, Suzuki Y, Oritani KE, Tomatsu S. (2017). Presentation and treatments for mucopolysaccharidosis type II (MPS II; Hunter syndrome). *Expert Opin Orphan Drugs* 5:295-307.

Superti-Furga, A., Unger, S., & Nosology Group of the International Skeletal Dysplasia Society. (2007). Nosology and classification of genetic skeletal disorders: 2006 revision. *American journal of medical genetics Part A*, 143(1), 1-18.

Takeda, K., Kou, I., Kawakami, N., Iida, A., Nakajima, M., Ogura, Y., ... & Ikegawa, S. (2017). Compound heterozygosity for null mutations and a common hypomorphic risk haplotype in *TBX6* causes congenital scoliosis. *Human mutation*, 38(3), 317-323.

Tomatsu S, Fukuda S, Masue M, Sukegawa K, Fukao T, Yamagishi A, Oritani T (1991). Morquio disease: isolation, characterization and expression of full-length cDNA for human N-acetylgalactosamine-6-sulfate sulfatase. *Biochem Biophys Res Commun* 181:677-683.

Tomatsu S, Montano A, Oikawa H, Rowan D, Smith M, Barrera L, Oritani T (2011). Mucopolysaccharidosis type IVA (Morquio A disease): clinical review and current treatment: a special review. *Curr Pharm Biotechnol* 12:931-945.

Tomatsu S, Montano AM, Nishioka T, Gutierrez MA, Pena OM, Tranda Firescu GG, Oori T (2005). Mutation and polymorphism spectrum of the GALNS gene in mucopolysaccharidosis IVA (Morquio A). *Hum Mutat* 26:500-512.

Towers, M., Wolpert, L., & Tickle, C. (2012). Gradients of signalling in the developing limb. *Current opinion in cell biology*, 24(2), 181-187.

Triggs Raine B, Salo TJ, Zhang H, Wicklow BA, Natowicz MR (1999). Mutations in *HYAL1*, a member of a tandemly distributed multigene family encoding disparate hyaluronidase

Turnpenny, P. D., Sloman, M., & Dunwoodie, S. (2017). Spondylocostal dysostosis, autosomal recessive. *GeneReviews®*[Internet].

Turnpenny, P. D., Sloman, M., & Dunwoodie, S. (2017). Spondylocostal dysostosis, autosomal recessive. *GeneReviews®*[Internet].

Ullah, A., Umair, M., Muhammad, D., Bilal, M., Lee, K., Leal, S. M., & Ahmad, W. (2018). A novel homozygous variant in *BMPRII* underlies acromesomelic dysplasia Hunter–Thompson type. *Annals of human genetics*, 82(3), 129-134.

Umair, M., Khan, S., & Ahmad, W. (2015). Homozygous sequence variants in the *NPR2* gene underlying Acromesomelic dysplasia Maroteaux type (AMDM) in consanguineous families. *Annals of Human Genetics*, 79(4), 238-244.

Valayannopoulos V, Nicely H, Harmatz P, Turbeville S (2010). Mucopolysaccharidosis vi. *Orphanet J Rare Dis* 5:1-20.

Valstar MJ, Ruijter G. J, Van Diggelen OP, Poorthuis BJ, Wijburg FA (2008). Sanfilippo syndrome: a mini-review. *J Inher Metab Dis* 31:240-252.

Vasques, G. A., Arnhold, I. J., & Jorge, A. A. (2014). Role of the natriuretic peptide system in normal growth and growth disorders. *Hormone Research in Paediatrics*, 82(4), 222-229.

Warman, M. L., Cormier-Daire, V., Hall, C., Krakow, D., Lachman, R., LeMerrer, M., ... & Superti-Furga, A. (2011). Nosology and classification of genetic skeletal disorders: 2010 revision. *American journal of medical genetics Part A*, 155(5), 943-968.

Wei, X., Thomas, N., Hatch, N. E., Hu, M., & Liu, F. (2017). Postnatal craniofacial skeletal development of female C57BL/6NCrl mice. *Frontiers in physiology*, 8, 697.

Wilkie, A. O., & Morriss-Kay, G. M. (2001). Genetics of craniofacial development and malformation. *Nature Reviews Genetics*, 2(6), 458-468.

Zanetti A, D'Avanzo F, AlSayed M, Brusius Facchin AC, Chien YH, Giugliani R, Tomanin R. (2021). Molecular basis of mucopolysaccharidosis IVA (Morquio A syndrome): A review and classification of GALNS gene variants and reporting of 68 novel variants. *Hum Mutat* 42:1384-1398.